

# Earth



# ArXiv

## Anthropogenic Impacts on Antibiotic Resistance Genes and Microbial Communities in Groundwater of Taopu Industrial Park, Shanghai

Xinran Liu<sup>\*, a, &</sup>, Yawen Song<sup>a, &</sup>, Yinping Miao<sup>a</sup>, Jian Wang<sup>a</sup>, Min Liu<sup>a</sup>, Ye Li<sup>a</sup>, Ye Huang<sup>a</sup>

<sup>a</sup>Key Laboratory of Geographic Information Science (Ministry of Education), School of Geographic Sciences, East China Normal University, Shanghai 200241, China

<sup>&</sup>These authors contributed equally to this work

**Peer review status:**

This is a non-peer-reviewed preprint submitted to EarthArXiv.

<sup>\*</sup>Corresponding Author:

Xinran Liu, Email: [xrliu@geo.ecnu.edu.cn](mailto:xrliu@geo.ecnu.edu.cn)

1                   **Anthropogenic Impacts on Antibiotic Resistance**  
2                   **Genes and Microbial Communities in Groundwater**  
3                   **of Taopu Industrial Park, Shanghai**

4  
5                   Xinran Liu<sup>\*, a, &</sup>, Yawen Song<sup>a, &</sup>, Yinping Miao<sup>a</sup>, Jian Wang<sup>a</sup>, Min Liu<sup>a</sup>, Ye  
6                   Huang<sup>a</sup>  
7

8                   <sup>a</sup>Key Laboratory of Geographic Information Science (Ministry of Education), School  
9                   of Geographic Sciences, East China Normal University, Shanghai 200241, China

10  
11                   <sup>&</sup>These authors contributed equally to this work  
12

13                   **Peer review status:**

14                   **This is a non-peer-reviewed preprint submitted to EarthArXiv.**

15  
16                   **\*Corresponding Author:**

17                   Xinran Liu, Email: [xrliu@geo.ecnu.edu.cn](mailto:xrliu@geo.ecnu.edu.cn)

19  
20  
21  
22

23      **Abstract**

24      Urban groundwater is increasingly recognized as an emerging reservoir and  
25      transport pathway for antibiotics, antibiotic-resistant bacteria (ARBs), and antibiotic  
26      resistance genes (ARGs), posing potential ecological and public-health risks. However,  
27      the distribution and transport mechanisms of antibiotics and ARGs in groundwater  
28      systems under complex anthropogenic pollution remain insufficiently understood. Here,  
29      we investigated groundwater in Shanghai's Taopu Industrial Park, a region  
30      characterized by multiple industrial contamination sources. Antibiotic concentrations  
31      were quantified using ultra-performance liquid chromatography–tandem mass  
32      spectrometry, while metagenomic sequencing and high-throughput quantitative PCR  
33      were employed to characterize ARG diversity and abundance and microbial community  
34      composition. Integrated analyses were performed to elucidate the distribution and  
35      transport patterns of antibiotics, microorganisms, and ARGs, and to identify key  
36      environmental drivers. Co-occurrence network analysis was further applied to infer  
37      potential ARB hosts.

38      Twenty antibiotics were detected in groundwater at concentrations ranging from  
39      24.1 to 1161.1 ng L<sup>-1</sup>, with sulfonamides dominating. Fluoroquinolones were more  
40      enriched in soil than groundwater, likely due to stronger sorption associated with their  
41      polar/ionic functional groups, whereas tetracyclines exhibited higher vertical mobility  
42      than sulfonamides. Antibiotic concentrations decreased exponentially with depth.  
43      Groundwater physicochemical parameters (dissolved organic carbon, salinity,

44 dissolved oxygen, and conductivity) together with co-occurring polycyclic aromatic  
45 hydrocarbons (PAHs) were the major determinants of antibiotic distribution.

46 Groundwater microbial communities were bacteria-dominated and of relatively  
47 low diversity, with Proteobacteria, Bacteroidetes, Actinobacteria, and Firmicutes as the  
48 major phyla. Actinobacteria occurred at higher relative abundance than in other  
49 industrial groundwater systems, likely reflecting selective pressure from the combined  
50 presence of antibiotics and PAHs, consistent with their roles in PAH degradation,  
51 antibiotic production, and ARG hosting. Redundancy analysis indicated that  
52 contaminants—particularly antibiotics and PAHs—were the primary drivers of  
53 microbial community structure, exceeding the effects of physicochemical parameters  
54 (pH, dissolved organic carbon, and dissolved oxygen).

55 The composition and relative abundance of 21 ARG types were highly similar  
56 between soil and groundwater, with multidrug, macrolide, glycopeptide, tetracycline,  
57 and peptide resistance genes predominating in both media, suggesting potential ARG  
58 exchange and migration across compartments. In groundwater, contaminants  
59 (especially antibiotics and PAHs) were the dominant determinants of ARG profiles,  
60 followed by microbial community composition, while mobile genetic elements and  
61 physicochemical conditions further facilitated ARG dissemination. Network analysis  
62 identified several shared potential ARG-hosting genera in soil and groundwater,  
63 indicating that ARB-mediated vertical transport may represent an important pathway  
64 for ARG contamination in groundwater.

65 Overall, this study reveals the coupled occurrence, transport behavior, and

66 environmental drivers of antibiotics, microbial communities, and ARGs in urban  
67 groundwater under anthropogenic influence. The findings highlight the need for  
68 integrated management strategies that reduce source pollutants and selective pressure  
69 to mitigate ARG dissemination in subsurface environments.

70

71 **Keywords:** Ultra-performance liquid chromatography–tandem mass spectrometry,  
72 Metagenomics, HT-qPCR, Antibiotics, ARGs, Groundwater

73

74

75

76 **1 Introduction**

77 Since their initial discovery in the 1920s, antibiotics—owing to their bactericidal  
78 or bacteriostatic effects—have fundamentally transformed modern medicine and  
79 animal husbandry, and are now among the most extensively used pharmaceuticals  
80 worldwide (Wang et al., 2015a). However, a large proportion of antibiotics  
81 administered to humans and animals are not fully absorbed or metabolized, with 30–  
82 90% of veterinary antibiotics excreted via animal manure (Pan et al., 2011). The  
83 widespread overuse of antibiotics, coupled with incomplete absorption and  
84 metabolism, has led to substantial antibiotic release into the environment. This has  
85 resulted in pervasive contamination of soil, water bodies, and the atmosphere, exerting  
86 selective pressure on environmental microorganisms and thereby accelerating the  
87 proliferation of ARBs and ARGs. These developments pose a significant threat to  
88 human health and ecosystem stability (Zhang et al., 2017a; Yi et al., 2019).

89 As a novel class of environmental contaminants, ARGs can be utilized by bacteria,  
90 undergoing rapid proliferation and dissemination through the growth of ARBs and  
91 horizontal gene transfer mechanisms. This enables the potential transfer of ARB from  
92 common environmental bacteria to those recognized as human pathogens, thereby  
93 seriously compromising antibiotic efficacy and posing a detrimental impact on public  
94 health (Pehrsson et al., 2016). Owing to the selective pressure exerted by antibiotics on  
95 ARGs, current research has predominantly focused on environmental media with  
96 known antibiotic sources, such as agricultural soils (Li et al., 2021), wastewater (Jong

97 et al., 2020), sewage sludge (Wei et al., 2018), various sediments (Chen et al., 2022a),  
98 and the atmosphere (He et al., 2020). However, existing studies indicate that other  
99 contaminants, including heavy metals (Li et al., 2022c) and organic pollutants  
100 (Azhogina et al., 2022), also facilitate the spread and dissemination of ARGs.  
101 Consequently, it is imperative to investigate the contamination levels and influencing  
102 factors of ARGs in industrial parks characterized by multiple pollutant sources.

103 Groundwater constitutes a critical component of the urban water cycle and water  
104 supply systems, and its quality is closely linked to ecological security and human health.  
105 Previous research on antibiotics and ARGs has predominantly focused on surface soils  
106 and surface water bodies (Das et al., 2021; Hao et al., 2021), often overlooking the  
107 impact of intensive anthropogenic activities in urban industrial parks on the deeper soil  
108 layers and groundwater systems. While the vadose zone can provide a degree of  
109 buffering capacity for groundwater quality, thereby slowing the migration of  
110 contaminants (Garcia-Galan et al., 2011), the adsorption efficiency of the soil-  
111 groundwater system is influenced by both soil properties (e.g., pH, organic matter  
112 content, and soil composition) and contaminant characteristics (e.g., acid dissociation  
113 constants and water solubility). To date, limited research exists on the migration of  
114 antibiotics and ARGs across different environmental media, especially between soil and  
115 groundwater. Therefore, this study investigates the distribution and transport of  
116 antibiotics and ARGs within the soil-groundwater continuum, aiming to provide data  
117 support and a scientific foundation for the prevention, control, and remediation of  
118 antibiotic and ARG contamination in groundwater.

119 Based on the aforementioned background, this study selects the Shanghai Taopu  
120 Industrial Park, characterized by typical composite pollution, as the research area, with  
121 groundwater as the primary focus. The aim is to elucidate the distribution patterns,  
122 migration processes, and key influencing factors of antibiotics and ARGs within the  
123 soil-groundwater system. The findings are expected to provide a scientific basis for the  
124 remediation and ecological restoration of groundwater contamination in the region, as  
125 well as offer theoretical support for systematically assessing the ecological risks and  
126 transport mechanisms of ARGs in complex pollution environments.

127

## 128 **2 Materials and methods**

### 129 **2.1 Study area and sampling**

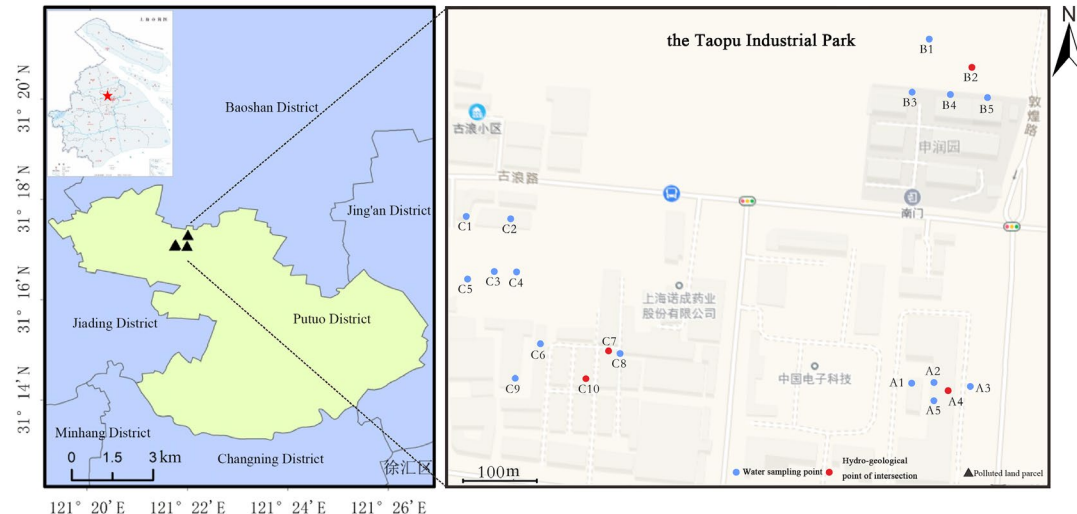
130 The Taopu Industrial Park is located in northwestern Shanghai and was established  
131 in the 1950s, with fine chemicals and pharmaceutical manufacturing historically  
132 serving as its leading industries. During its early development, the area hosted a  
133 concentration of pharmaceutical, chemical, pen manufacturing, and textile enterprises,  
134 resulting in a series of environmental issues. While existing studies have examined  
135 contamination by heavy metals and persistent organic pollutants in the region (Lu et al.,  
136 2006), the potential antibiotic and antibiotic resistance gene (ARG) pollution associated  
137 with the historical presence of numerous pharmaceutical companies—such as Shanghai  
138 Fangda Pharmaceutical Co., Ltd., Shanghai Jiuzhoutong Pharmaceutical Co., Ltd., and  
139 Shanghai Schering-Plough Pharmaceutical Co., Ltd.—has not yet been systematically

140 reported.

141

142 **2.2 Sample collection**

143 Groundwater sampling was conducted in the Taopu Industrial Park, Shanghai,  
144 between October and November 2020 (Fig. 1). An integrated soil-groundwater  
145 sampling device equipped with a bailer tube (Model: QY-60, Xitan, Jiangsu) was used  
146 to collect a total of 20 groundwater samples, labeled A1–5, B1–5, and C1–10. At each  
147 sampling point, 4 liters of groundwater were collected. Immediately after collection,  
148 the samples were stored in polyethylene bottles, appropriately labeled, placed in light-  
149 proof insulated containers with ice packs, and transported to the laboratory within 24  
150 hours, where they were refrigerated at 4°C. During the pretreatment process, each water  
151 sample was divided into two portions: one portion was filtered through a 0.22 µm  
152 membrane to collect suspended particulate matter retained on the filter for subsequent  
153 DNA extraction; the other portion was filtered through a 0.45 µm membrane, and the  
154 filtrate was preserved for the analysis of antibiotics, PAHs, and physicochemical water  
155 quality indicators.



156  
157 Fig. 1 Sampling sites in Taopu industrial park in Shanghai.  
158  
159

160 **2.3 Analyses of physicochemical properties, metals and PAHs**

161 On-site measurements of groundwater temperature, dissolved oxygen (DO), pH,  
162 and conductivity were performed using a portable multi-parameter water quality  
163 analyzer (Multi 3630 IDS, WTW, Germany). Concentrations of dissolved organic  
164 carbon (DOC) and total dissolved nitrogen (TDN) were determined by a total organic  
165 carbon analyzer (TOC-V, Shimadzu, Japan). Prior to analysis, water samples were  
166 diluted 100-fold, with ultrapure water serving as the blank control.

167 Six heavy metals commonly associated with anthropogenic activities and  
168 potentially linked to the presence of ARGs in the environment—Mn, Cu, Zn, Ni, Pb,  
169 and Cr—were analyzed following a modified version of the method described by Yang  
170 et al. (2016a). Groundwater samples were filtered through 0.45  $\mu\text{m}$  aqueous syringe  
171 filters (polyethersulfone membrane) and subsequently analyzed using inductively  
172 coupled plasma optical emission spectrometry (ICP-OES). The spike recovery rates for

173 the target metals ranged from 64.4% to 92.7%.

174 The analysis of 16 PAHs in groundwater samples followed a previously

175 established method (Wu et al., 2018). The specific procedure is summarized as follows:

176 one liter of filtered water sample was spiked with 100 ng of deuterated terphenyl as a

177 recovery indicator. PAHs were enriched and purified using an HC-18 solid-phase

178 extraction cartridge (200 mg, 6 mL, CNW). The PAH fraction was eluted with 15 mL

179 of a hexane–dichloromethane mixed solvent (3:7, v/v). The eluate was dehydrated with

180 anhydrous sodium sulfate (high-purity grade) and then concentrated using rotary

181 evaporation. The solvent was subsequently replaced with hexane and concentrated

182 again to 1–2 mL before being transferred into a GC vial. After precise volume

183 adjustment to 1 mL under a gentle nitrogen stream, 20  $\mu$ L of an internal standard

184 solution (10 mg/L) was added. The concentration of PAHs was determined using a gas

185 chromatography–mass spectrometry system (GC–MS, Agilent 7890A/5977B, USA).

186 The recoveries of target PAHs ranged from 60.1% to 125.5%; all sample concentrations

187 were corrected based on recovery rates. For every ten samples, one method blank (using

188 deionized water as a sample substitute) was processed, and the concentrations of target

189 analytes in all blank samples were below the instrumental detection limit. In addition,

190 25% of the samples were randomly selected for triplicate analysis, with relative

191 standard deviations all below 15.0%.

192

193 **2.4 Quantification of Antibiotics**

194 **2.4.1 Antibiotic analysis**

195 During the pretreatment step, 800 mL of membrane-filtered water sample was  
196 measured and transferred into an amber glass bottle. A total of 40 ng of surrogate  
197 standard (tetracycline-D6, TC-D6) was spiked into the sample. The pH of the sample  
198 was adjusted to 5.0 using high-purity hydrochloric acid and sodium hydroxide solution.  
199 Subsequently, analytical-grade ethylenediaminetetraacetic acid disodium salt (EDTA-  
200 2Na) was added to achieve a final concentration of 1.0 g/L. After thorough mixing, the  
201 sample was left to stand for 1 hour to allow chelation of interfering metal ions, followed  
202 by loading onto a solid-phase extraction cartridge.

203 Prior to sample loading, the solid-phase extraction cartridge was sequentially  
204 preconditioned with 5 mL of methanol and 5 mL of ultrapure water at a flow rate of 1  
205  $\text{mL}\cdot\text{min}^{-1}$ . During the enrichment process, the water sample was passed through the  
206 cartridge at a controlled flow rate of 5  $\text{mL}\cdot\text{min}^{-1}$ . After enrichment, the cartridge was  
207 rinsed with 10 mL of ultrapure water and dried under vacuum for at least 30 minutes.  
208 Target analytes were then eluted using 10 mL of a methanol–acetonitrile mixture (1:1,  
209 v/v). The eluate was concentrated by rotary evaporation to a volume of 1–2 mL. The  
210 solvent was then exchanged to methanol using 8 mL of methanol and concentrated  
211 again to 1–2 mL. The concentrate was transferred to an injection vial and evaporated  
212 under a gentle nitrogen stream to 0.5 mL. Finally, the sample was diluted to 1 mL with  
213 0.02  $\text{mol}\cdot\text{L}^{-1}$  formic acid solution, filtered, and prepared for instrumental analysis.

214 This study selected 20 target antibiotic standards covering five major classes:

215 chloramphenicols (CPs), fluoroquinolones (FQs), macrolides (MLs), sulfonamides  
216 (SAs), and tetracyclines (TCs). The quantification of target antibiotics in the samples  
217 was performed using an ultra-performance liquid chromatography-tandem mass  
218 spectrometry system (UPLC-MS/MS, Waters Corp., Manchester, UK).

219

220 **2.4.2 Quality assurance/quality control**

221 A rigorous quality control and quality assurance (QC/QA) protocol was  
222 implemented throughout the experimental procedure. The specific measures included:  
223 (1) spiking 40 ng of TC-D6 as a recovery indicator into the groundwater samples, with  
224 the recoveries of the 20 target antibiotics ranging from 40.1% to 114.9%; (2) conducting  
225 method blank tests using deionized water in place of samples, and the limits of detection  
226 for target compounds were between 0.00 and 0.53 ng/L; and (3) performing triplicate  
227 analyses on 30% of randomly selected samples, all of which exhibited relative standard  
228 deviations below 15.0%.

229

230 **Table 1 Basic information of 20 antibiotics**

| Types of antibiotics | Chemical formula   | CAS Number | Molecular weight |
|----------------------|--|------------|------------------|
| Sulfadiazine         | C <sub>10</sub> H <sub>10</sub> N <sub>4</sub> O <sub>2</sub> S            | 68-35-9    | 250.28           |
| Sulfapyridine        | C <sub>11</sub> H <sub>11</sub> N <sub>3</sub> O <sub>2</sub> S            | 144-83-2   | 249.29           |
| Sulfamethoxazole     | C <sub>10</sub> H <sub>11</sub> N <sub>3</sub> O <sub>3</sub> S            | 723-46-6   | 253.28           |
| Sulfathiazole        | C <sub>9</sub> H <sub>9</sub> N <sub>3</sub> O <sub>2</sub> S <sub>2</sub> | 72-14-0    | 255.32           |
| Sulfamerazine        | C <sub>11</sub> H <sub>12</sub> N <sub>4</sub> O <sub>2</sub> S            | 127-79-7   | 264.30           |
| Sulfamethazine       | C <sub>12</sub> H <sub>14</sub> N <sub>4</sub> O <sub>2</sub> S            | 200-346-4  | 278.33           |
| Sulfaquinoxaline     | C <sub>14</sub> H <sub>12</sub> N <sub>4</sub> O <sub>2</sub> S            | 59-40-5    | 300.34           |
| Norfloxacin          | C <sub>16</sub> H <sub>18</sub> FN <sub>3</sub> O <sub>3</sub>             | 70458-96-7 | 319.33           |
| Ciprofloxacin        | C <sub>17</sub> H <sub>18</sub> FN <sub>3</sub> O <sub>3</sub>             | 85721-33-1 | 331.34           |
| Enrofloxacin         | C <sub>19</sub> H <sub>22</sub> FN <sub>3</sub> O <sub>3</sub>             | 93106-60-6 | 359.40           |
| Oflloxacin           | C <sub>18</sub> H <sub>20</sub> FN <sub>3</sub> O <sub>4</sub>             | 82419-36-1 | 361.37           |
| Tetracycline         | C <sub>22</sub> H <sub>24</sub> N <sub>2</sub> O <sub>8</sub>              | 60-54-8    | 444.45           |

|                      |   |            |        |
|----------------------|---|------------|--------|
| Oxytetracycline      | C <sub>22</sub> H <sub>24</sub> N <sub>2</sub> O <sub>9</sub>                 | 79-57-2    | 460.43 |
| Doxycyclinehydyclate | C <sub>22</sub> H <sub>24</sub> N <sub>2</sub> O <sub>8</sub>                 | 564-25-0   | 444.44 |
| Chlorotetracycline   | C <sub>22</sub> H <sub>23</sub> ClN <sub>2</sub> O <sub>8</sub>               | 57-62-5    | 478.88 |
| Erythromycin         | C <sub>37</sub> H <sub>67</sub> NO <sub>13</sub>                              | 114-07-8   | 733.94 |
| Roxithromycin        | C <sub>41</sub> H <sub>76</sub> N <sub>2</sub> O <sub>15</sub>                | 80214-83-1 | 837.05 |
| Chloramphenicol      | C <sub>11</sub> H <sub>12</sub> C <sub>12</sub> N <sub>2</sub> O <sub>5</sub> | 56-75-7    | 323.13 |
| Thiamphenicol        | C <sub>12</sub> H <sub>15</sub> C <sub>12</sub> NO <sub>5</sub> S             | 15318-45-3 | 356.22 |
| Florfenicol          | C <sub>12</sub> H <sub>14</sub> C <sub>12</sub> FNO <sub>4</sub> S            | 73231-34-2 | 358.21 |

231

232 **2.5 DNA extraction, metagenomic sequencing, and gene annotation**

233 Two liters of groundwater were filtered through a 0.22 µm mixed cellulose ester  
 234 membrane (Sangon Biotech, Shanghai) to collect particulate matter retained on the  
 235 filter for DNA extraction. The filter membrane was aseptically cut into small pieces  
 236 using sterilized scissors and forceps, then transferred into a lysis tube. DNA extraction  
 237 was performed using the FastDNA® Spin Kit (MP Biomedicals, USA) strictly  
 238 following the manufacturer's protocol. The extracted DNA was assessed for quality and  
 239 concentration using a microvolume spectrophotometer (Thermo Fisher Scientific,  
 240 USA), ensuring that the OD260/280 ratio fell within 1.8–2.0 to meet the requirements  
 241 for subsequent analyses. Finally, the extracted DNA was aliquoted: one portion was  
 242 used for metagenomic sequencing, and another portion was reserved for high-  
 243 throughput quantitative PCR (HT-qPCR) analysis. All DNA aliquots were stored at -  
 244 20°C to prevent degradation.

245 DNA extracted from the groundwater samples was shipped on dry ice to Shanghai  
 246 Majorbio Bio-pharm Technology Co., Ltd. (Shanghai, China) for sequencing. Extracted  
 247 DNA was fragmented to approximately 400 bp using a Covaris M220 (Gene Company  
 248 Limited, China) for paired-end library preparation. Sequencing was performed on an

249 Illumina NovaSeq platform, and raw reads were saved in FASTQ format. Quality  
250 control was conducted using fastp (Chen et al., 2018) to obtain high-quality clean data,  
251 ensuring the reliability of subsequent analyses (<https://github.com/OpenGene/fastp>,  
252 version 0.20.0). Clean reads were assembled into contigs using MEGAHIT (Li et al.,  
253 2015b) (<https://github.com/voutcn/megahit>, version 1.1.2). Open reading frames  
254 (ORFs) were predicted from the assembled contigs with MetaGene (Version 2.10)  
255 (Noguchi et al., 2006) (<http://metagene.cb.k.u-tokyo.ac.jp/>). The predicted genes were  
256 clustered using CD-HIT (Fu et al., 2012) to construct a non-redundant gene catalog  
257 (<http://www.bioinformatics.org/cd-hit/>). Abundance information of genes in each  
258 sample was obtained by aligning high-quality reads to the non-redundant gene catalog  
259 using SOAPaligner (Li et al., 2009) with a default identity threshold of 95%  
260 (<http://soap.genomics.org.cn/>). The non-redundant gene set was functionally annotated  
261 against the NR database (<http://www.diamondsearch.org/index.php>, version 0.8.35)  
262 using DIAMOND (Buchfink et al., 2015; Buchfink et al., 2021) with the blastp  
263 algorithm and an E-value cutoff of 1e-5. ARGs were annotated using the  
264 Comprehensive Antibiotic Resistance Database (CARD) (Jia et al., 2017)  
265 (<https://card.mcmaster.ca/>, version 0.8.35) under the same parameters. Mobile genetic  
266 elements (MGEs) were identified by alignment to a curated MGE database (Parnanen  
267 et al., 2018) (<https://github.com/KatariinaParnanen/MobileGeneticElementDatabase>,  
268 Version 2.1) using blastp with an E-value  $\leq$  1e-5. All sequencing data generated in this  
269 study have been deposited in the NCBI Sequence Read Archive (SRA) under  
270 BioProject accession number PRJNA945244.

271

272 **2.6 Statistical analyses**

273 For data analysis and visualization, this study employed a variety of statistical and  
274 graphical tools. Statistical description and preprocessing of data on antibiotic resistance  
275 genes, heavy metals, and physicochemical parameters were performed using SPSS 19.0  
276 (SPSS Inc., Chicago, IL, USA). To evaluate the direct and indirect effects of soil  
277 properties, pollutants, microbial abundance and diversity, and mobile genetic elements  
278 (MGEs) on the spatial distribution of ARGs, a structural equation model (SEM) was  
279 constructed.

280 Within the R environment, redundancy analysis (RDA) and variation partitioning  
281 analysis (VPA) were conducted using the Vegan package to quantify the contributions  
282 of environmental factors to the variation in ARG distribution. Spearman correlation  
283 analysis was performed with the Hmisc package to identify co-occurrence patterns  
284 among ARG subtypes, microbial taxa, and MGEs, applying selection thresholds of  
285 Spearman's rho  $> 0.8/0.6$  and a p-value  $< 0.01$ . Network visualization was generated  
286 using Gephi 9.1. The spatial distribution map of the study area and sampling points was  
287 created with ArcGIS 10.6. All bar charts, line graphs, and pie charts were produced in  
288 OriginPro 2019b.

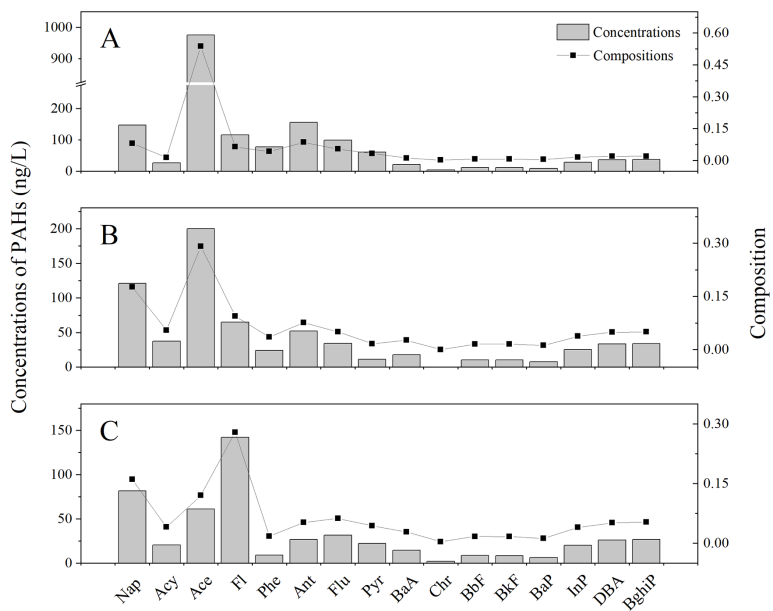
289

290 **3 Results**

291 **3.1 Physicochemical properties and PAH concentrations**

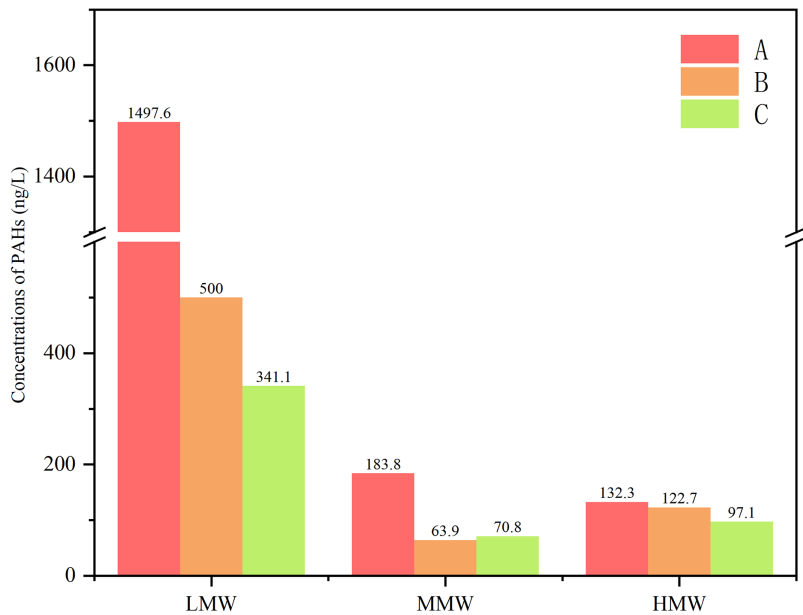
292 Analysis of groundwater monitoring data from the Taopu Industrial Park in  
293 Shanghai reveals the following characteristics: the pH of the 20 collected samples  
294 ranged from 6.8 to 9.5, with an average of 7.4; dissolved oxygen (DO) concentrations  
295 varied between 2.3 and 11.8 mg/L, with the lowest value recorded at site A2; salinity  
296 ranged from 0.3‰ to 1.4‰; electrical conductivity, dissolved organic carbon (DOC),  
297 and total nitrogen (TN) exhibited significant variation, with ranges of 805.0–3060.0  
298  $\mu\text{S}/\text{cm}$ , 3.7–34.5 mg/L, and 1.2–35.8 mg/L, respectively; the average groundwater  
299 temperature was 19.4°C, with minimal variation observed within the same sampling  
300 area.

301 As illustrated in Fig. 3, significant spatial variability was observed in the  
302 concentrations of PAHs in the groundwater samples from the Taopu Industrial Park.  
303 The highest total PAHs concentration was recorded at site A2, reaching  $5172.8 \text{ ng L}^{-1}$ ,  
304 while the lowest was observed at site C7 ( $250.5 \text{ ng L}^{-1}$ ), with an average concentration  
305 of  $899.1 \text{ ng L}^{-1}$ . Compared to groundwater in other regions both domestically and  
306 internationally, the total concentration of the 16 PAHs in this area is significantly higher  
307 than those reported for Taiyuan, China ( $135 \text{ ng L}^{-1}$ ), Jharkhand, India ( $22 \text{ ng L}^{-1}$ ), and  
308 Shenyang New District, Liaoning, China ( $467 \text{ ng L}^{-1}$ ). It is comparable to the level  
309 reported for Rawalpindi, Pakistan ( $763 \text{ ng L}^{-1}$ ), indicating that the groundwater in this  
310 industrial park is subjected to a relatively high level of PAHs contamination (Fig. 2).



312

313        Fig. 2 Concentrations and composition of Individual PAHs in Groundwater in Taopu industrial  
 314        park in Shanghai.



315

316        Fig. 3 Concentration of PAHs in Groundwater in Taopu industrial park in Shanghai.  
 317

318 3.2 The distribution of antibiotics in groundwater

319 3.2.1 The concentration of antibiotics in groundwater

320 Analysis of five major classes of antibiotics in 20 groundwater samples from the

321 Taopu Industrial Park revealed that the total concentration of the 20 target antibiotics

322 ranged from 24.1 to 1161.1 ng L<sup>-1</sup>, with an average concentration of 263.3 ng L<sup>-1</sup>.

323 Compared with domestic and international studies, the antibiotic contamination in the

324 groundwater of this industrial park is at a moderate level.

325 Sulfonamides (SAs) exhibited the highest concentration among all antibiotic

326 classes, accounting for 68.8% of the total antibiotic concentration, followed by

327 fluoroquinolones (FQs, 12.1%), tetracyclines (TCs, 10.7%), chloramphenicols (CPs,

328 7.0%), and macrolides (MLs, 1.4%). This distribution pattern is consistent with findings

329 from previous studies (Chen et al., 2017d; Ma et al., 2021). The strong mobility and

330 low degradation rates of SAs likely contribute to their enrichment in groundwater (Fig.

331 4).

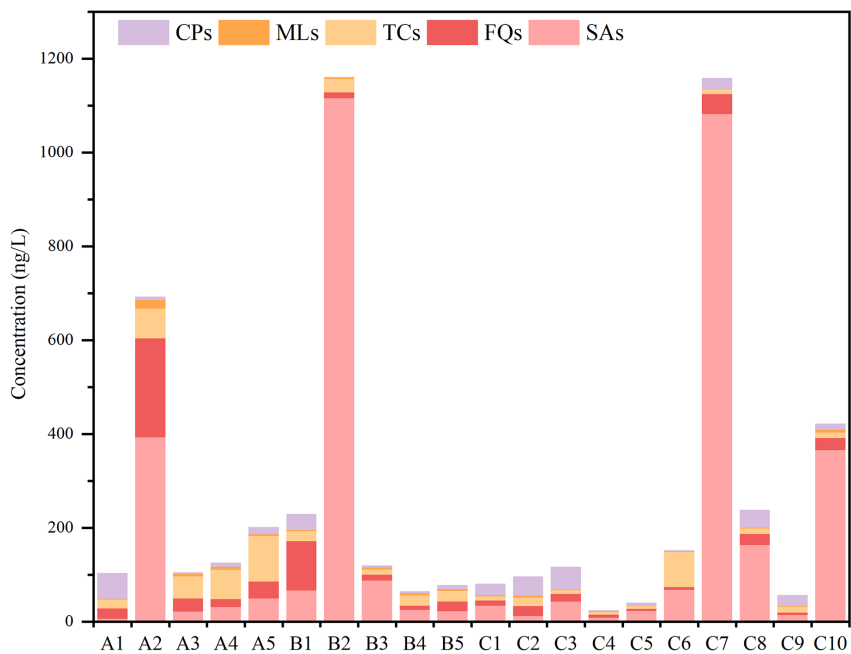
332 It is noteworthy that all 20 target antibiotics were detected in every sample. Among

333 them, two SAs (SD and SMT), one FQ (NFC), four TCs (TC, DXC, OTC, and CTC),

334 two MLs (ETM and RTM), and one CP (CAP) were detected in 100% of the samples.

335

336



337

338 Fig. 4 The concentration of antibiotics in groundwater in Taopu industrial park in Shanghai.  
339

340 3.2.2 Distribution and Transport of Antibiotics in the Soil-Groundwater System

341       Driven by anthropogenic activities, a significant portion of antibiotics used in  
342       human medicine, animal husbandry, and agriculture enters various environmental  
343       compartments through direct or indirect pathways due to incomplete absorption and  
344       utilization (Huang et al., 2019b; Norback et al., 2019; Seyoum et al., 2021).

345       Soil serves as a major reservoir for environmental antibiotics. Once introduced  
346       into soil, antibiotics undergo processes such as adsorption/desorption, degradation, and  
347       bioaccumulation, resulting in distinct distribution and transport patterns along the soil  
348       profile (Qiao et al., 2018; Zhao et al., 2017). In urban settings, intensive human  
349       activities further influence the distribution and migration of pollutants within the soil

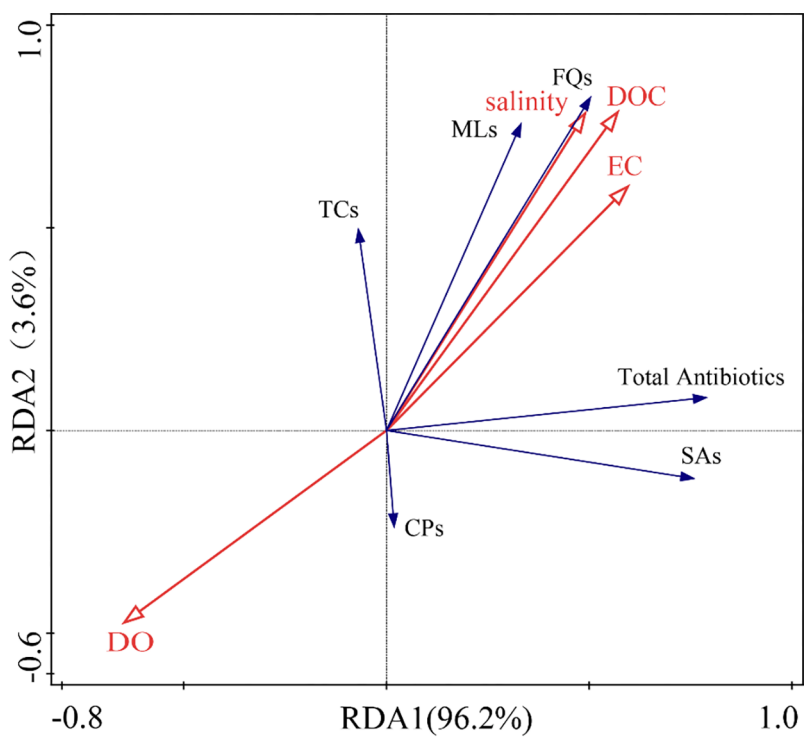
350 profile (Bu et al., 2009).

351       Antibiotics released from anthropogenic activities are widely distributed in soil  
352 and groundwater environments. In our previous study conducted in the same area, the  
353 concentrations of total antibiotics, tetracyclines (TCs), and fluoroquinolones (FQs) in  
354 soil cores followed an exponential decay model, decreasing with soil depth. In contrast,  
355 the distribution of sulfonamides (SAs), macrolides (MLs), and chloramphenicols (CPs)  
356 along the soil profile did not conform to an exponential decay pattern, which may be  
357 attributed to their physicochemical properties, chemical degradation, and  
358 biodegradation. Although the vadose zone soil provides some retardation of antibiotic  
359 migration, the low temperatures, anoxic conditions, and lack of light in groundwater  
360 environments slow down antibiotic degradation, leading to their accumulation.  
361 Antibiotic contamination in the study area's groundwater has reached a moderate level,  
362 with sulfonamides (SAs)—a highly mobile antibiotic class—being the dominant  
363 component.

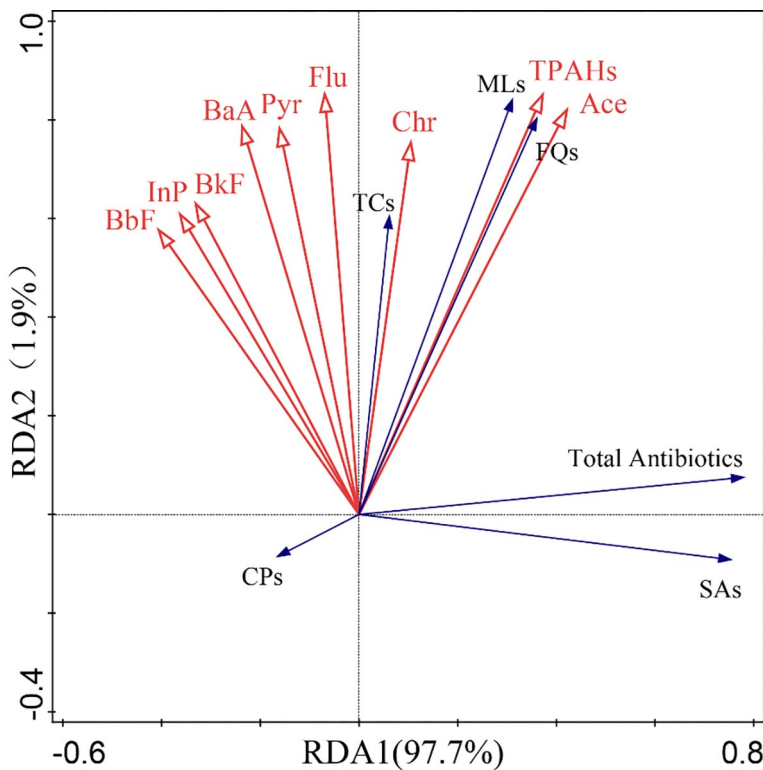
364       The distribution of antibiotics in groundwater is also significantly influenced by  
365 dissolved organic carbon (DOC), salinity, and dissolved oxygen (DO). Furthermore, the  
366 elevated levels of PAHs in the industrial park groundwater play an important role in  
367 shaping antibiotic distribution. Eight PAHs, including Ace, Flu, Pyr, BaA, Chr, BbF,  
368 BkF, and InP, as well as total PAHs (TPAH), showed significant correlations with  
369 antibiotic concentrations. This may be due to the selective pressure exerted by PAHs,  
370 which promotes the proliferation of antibiotic-producing microbial strains while  
371 simultaneously suppressing the degradation functions of PAH-degrading bacteria,

372 thereby facilitating the long-term coexistence of both pollutant groups in the  
373 environment.

374 This study demonstrates that the migration and transformation of antibiotics in the  
375 soil-groundwater system result from the combined effects of anthropogenic discharge,  
376 intrinsic antibiotic properties, environmental media characteristics, and regional  
377 composite pollution. Therefore, effective pollution prevention and control require an  
378 integrated strategy that accounts for cross-media interactions and multi-factor  
379 synergistic management (Fig. 5 and Fig. 6).



380  
381 Fig. 5 Redundancy analysis (RDA) showing the influence from physical and chemical  
382 properties on antibiotics in groundwater samples.



383

384 Fig. 6 Redundancy analysis (RDA) showing the influence from PAHs contents on antibiotics in  
 385 groundwater samples.

386

387

388 **3.3 ARG and MGE profiles**

389 Based on antibiotic class, the ARGs detected via high-throughput quantitative  
 390 PCR (HT-qPCR) in this study were categorized into eight groups: sulfonamide,  
 391 tetracycline, multidrug, fluoroquinolone, macrolide-lincosamide-streptogramin B  
 392 (MLSB),  $\beta$ -lactam, aminoglycoside, and other resistance genes.

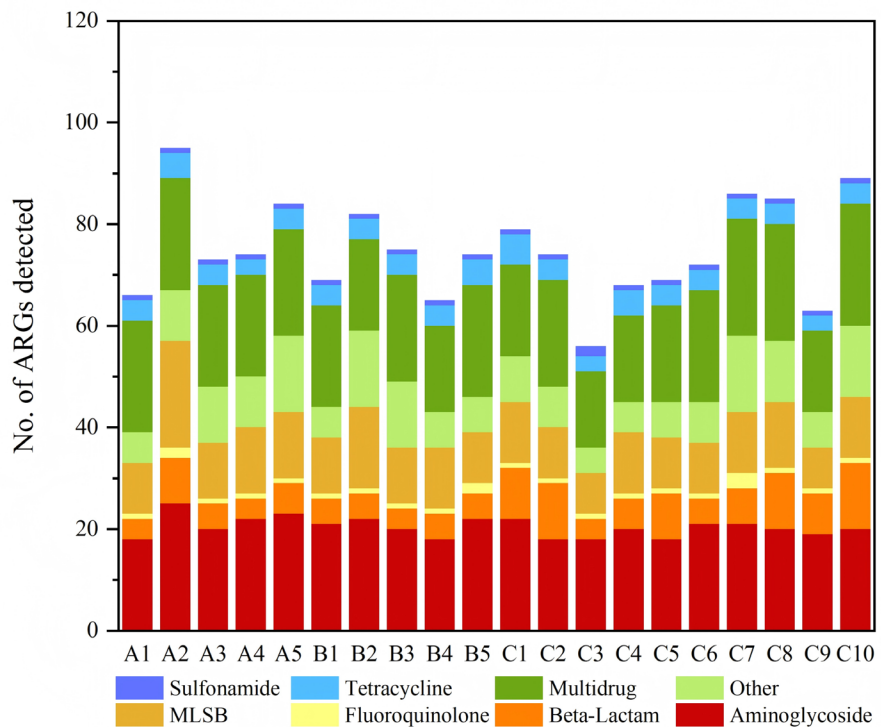
393 Fig. 7 presents the number of distinct antibiotic resistance gene (ARG) subtypes  
 394 detected via high-throughput quantitative PCR (HT-qPCR) across 20 groundwater  
 395 samples. A total of 163 different ARG subtypes were identified, with their counts  
 396 varying moderately among samples, ranging from 56 to 95 subtypes per sample and  
 397 averaging 75 subtypes. The composition of the eight ARG classes was generally

398 consistent across all samples. Among them, aminoglycoside and multidrug resistance  
399 genes were the most abundant in terms of subtype diversity, with counts ranging from  
400 18–25 and 15–24 subtypes, respectively.

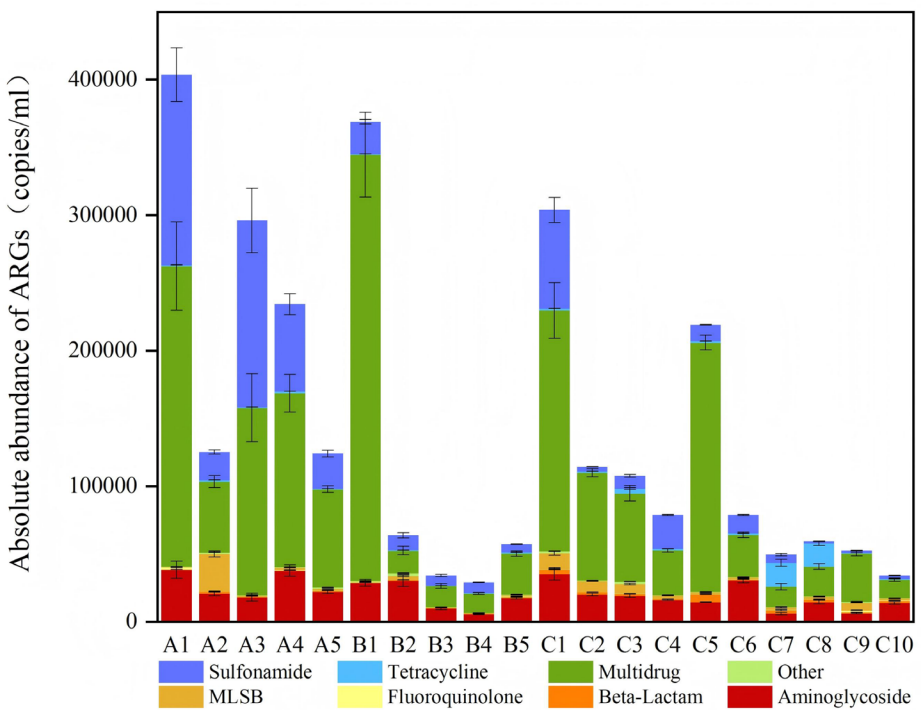
401 The absolute and relative abundances of the eight ARG classes in each  
402 groundwater sample are shown in Fig. 8. The absolute abundance of ARGs exhibited  
403 considerable variation, ranging from  $2.9 \times 10^4$ – $4.0 \times 10^5$  copies/mL, with an average of  
404  $1.4 \times 10^5$  copies/mL. In contrast, the relative abundance of ARGs showed less variability,  
405 ranging from 0.1 to 1.1. In terms of compositional distribution, multidrug resistance  
406 genes accounted for the highest proportion across all samples (3.3–77.9%), followed  
407 by aminoglycoside resistance genes (6.1–47.6%) and sulfonamide resistance genes  
408 (0.3–34.8%). The remaining five ARG classes contributed comparatively smaller  
409 proportions.

410 Compared to other studies that employed the high-throughput quantitative PCR  
411 (HT-qPCR) method to quantify ARGs in aquatic environments, the absolute abundance  
412 of ARGs in the groundwater of this study area is higher than that reported in household  
413 tap water from Zhangzhou, China ( $1.8 \times 10^7$  copies/L) (Huang et al., 2021) and  
414 aquaculture pond water in Huzhou, China ( $1.2 \times 10^7$  copies/L) (Tiimub et al., 2022).  
415 Conversely, it is lower than the levels found in the Houxi River, Xiamen, China  
416 ( $1.2 \times 10^{10}$  copies/L) (Zhou et al., 2020) and the drinking water source of the Jiulong  
417 River in Zhangzhou, China ( $1.9 \times 10^{10}$  copies/L) (Huang et al., 2021). The ARG  
418 abundance in this study is comparable to that observed in reservoir surface water in  
419 southeastern China ( $2.2 \times 10^6$ – $4.5 \times 10^8$  copies/L) (Fang et al., 2022) and summer

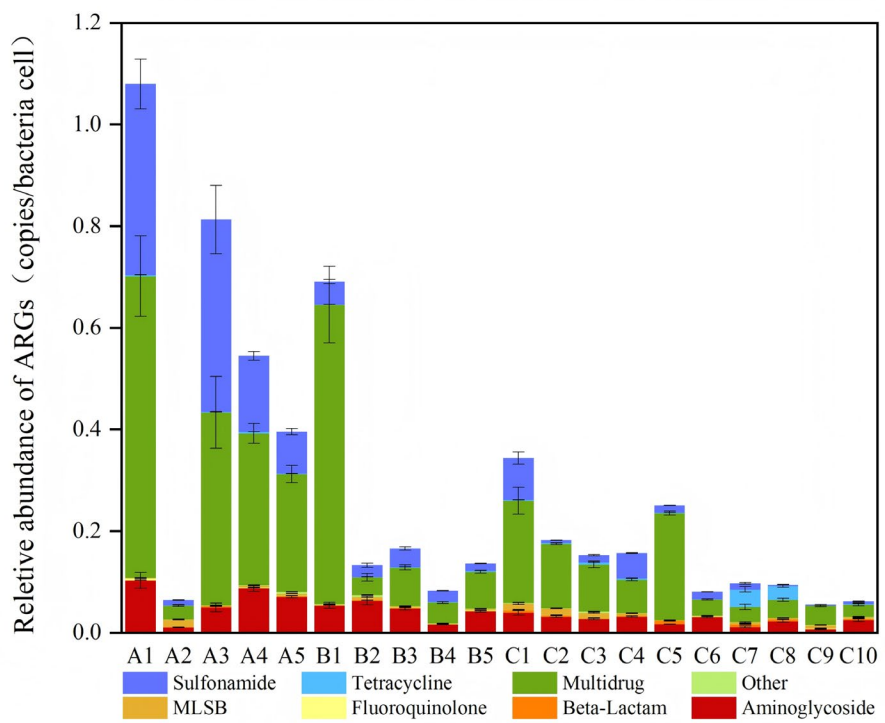
420 inflowing river water of Taihu Lake, China (6.17–9.47 Log<sub>10</sub> copies/L) (Fernanda et al.,  
421 2022), indicating a moderate level of contamination.



422  
423 Fig. 7 The total number of ARGs detected in groundwater samples.  
424



425



426

427 Fig. 8 Absolute abundance (a) and relative abundance (b) of ARGs detected in groundwater  
428 samples.

429

430 Building upon the HT-qPCR method, we employed metagenomic sequencing to  
431 conduct a comprehensive analysis of ARGs in the groundwater of the study area. Fig.  
432 9 illustrates the number of detected ARG subtypes and their normalized abundance  
433 across 20 groundwater samples using metagenomic sequencing.

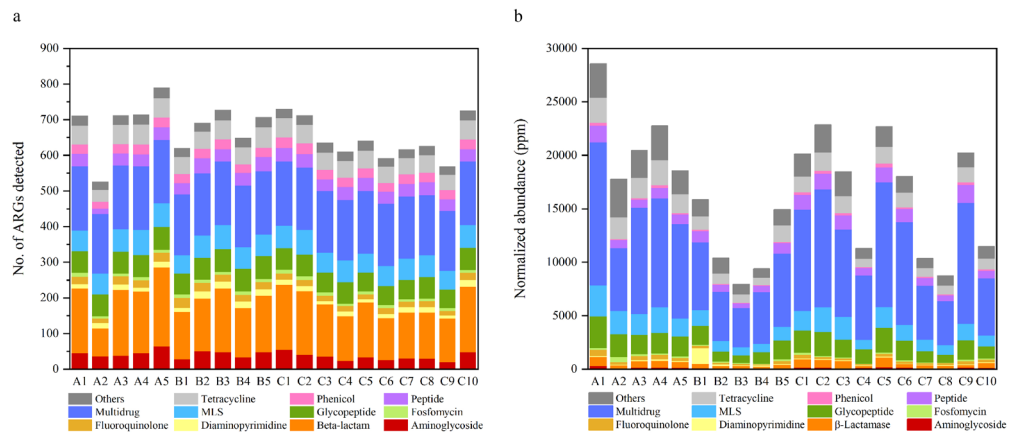
434 A total of 1,139 distinct ARG subtypes were identified in the 20 groundwater  
435 samples. The number of ARG subtypes per sample varied slightly, ranging from 526 to  
436 790, with an average of 665 subtypes (Fig. 9a). Among these, multidrug resistance  
437 genes were the most abundant in terms of subtype diversity, ranging from 167 to 180  
438 subtypes, followed by  $\beta$ -lactam resistance genes (78–222 subtypes) and glycopeptide  
439 resistance genes (52–65 subtypes).

440 As shown in Fig. 9b, the total normalized abundance of the 21 ARG classes varied  
441 substantially across samples, ranging from 7,951.8 to 28,548.9 ppm, with an average  
442 of 16,545.2 ppm. The top 10 most abundant ARG subtypes in the groundwater samples  
443 were macB, evgS, tetA(58), msbA, novA, mtrA, baeS, cpxA, oleC, and  
444 Sris\_parY\_AMU. Among these, macB was the most dominant, accounting for an  
445 average of 5.7% of the total ARG abundance, followed by evgS (5.4%) and tetA(58)  
446 (3.1%).

447 Among the 21 classes of ARGs detected in groundwater, multidrug resistance  
448 genes accounted for the highest proportion, ranging from 33.0% to 55.8%, followed by  
449 glycopeptide resistance genes (8.4–12.0%), macrolide resistance genes (7.7–12.4%),  
450 tetracycline resistance genes (6.8–11.6%), and peptide resistance genes (3.7–8.4%).  
451 This distribution pattern is consistent with findings from previous studies (Yang et al.,

452 2018) (Fig. 9b).

453



454

455

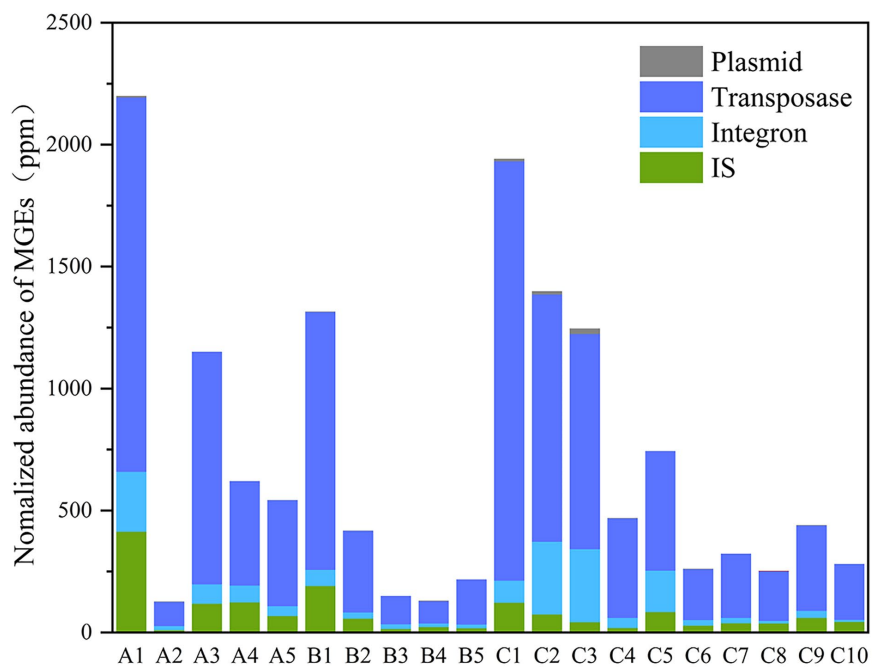
456 Fig. 9 The total number (a) and normalized abundance (b) of ARGs detected in groundwater  
457 samples

458

459 A total of 554 mobile genetic elements (MGEs) were identified across the 20  
460 groundwater samples, comprising 370 transposons, 133 insertion sequences, 48  
461 integrons, and 3 plasmids. The normalized abundance of MGEs ranged from 127.0 to  
462 2199.3 ppm, with an average value of 711.6 ppm (Fig. 10). Among the different MGE  
463 categories, transposons exhibited the highest relative abundance, accounting for 65.9%  
464 to 88.5% of the total MGE composition.

465

466



467

468       Fig. 10 Normalized abundance of MGEs in groundwater samples.

469

470       **3.4 Profiles of host bacteria of ARGs and potential human pathogens**

471       Across the 20 groundwater samples examined in this study, microorganisms  
 472 belonging to five distinct domains were detected. Bacteria constituted the dominant  
 473 microbial group, with their standardized relative abundance ranging from 74.8% to  
 474 99.8%. These were followed, in descending order of abundance, by Archaea (0.0–  
 475 12.1%), Eukaryota (0.0–11.8%), Viruses (0.0–3.4%), and unclassified microorganisms  
 476 (0.0–0.4%). Further taxonomic analysis revealed that the bacterial community  
 477 encompassed 153 phyla, 245 classes, 421 orders, 830 families, and 3538 genera.

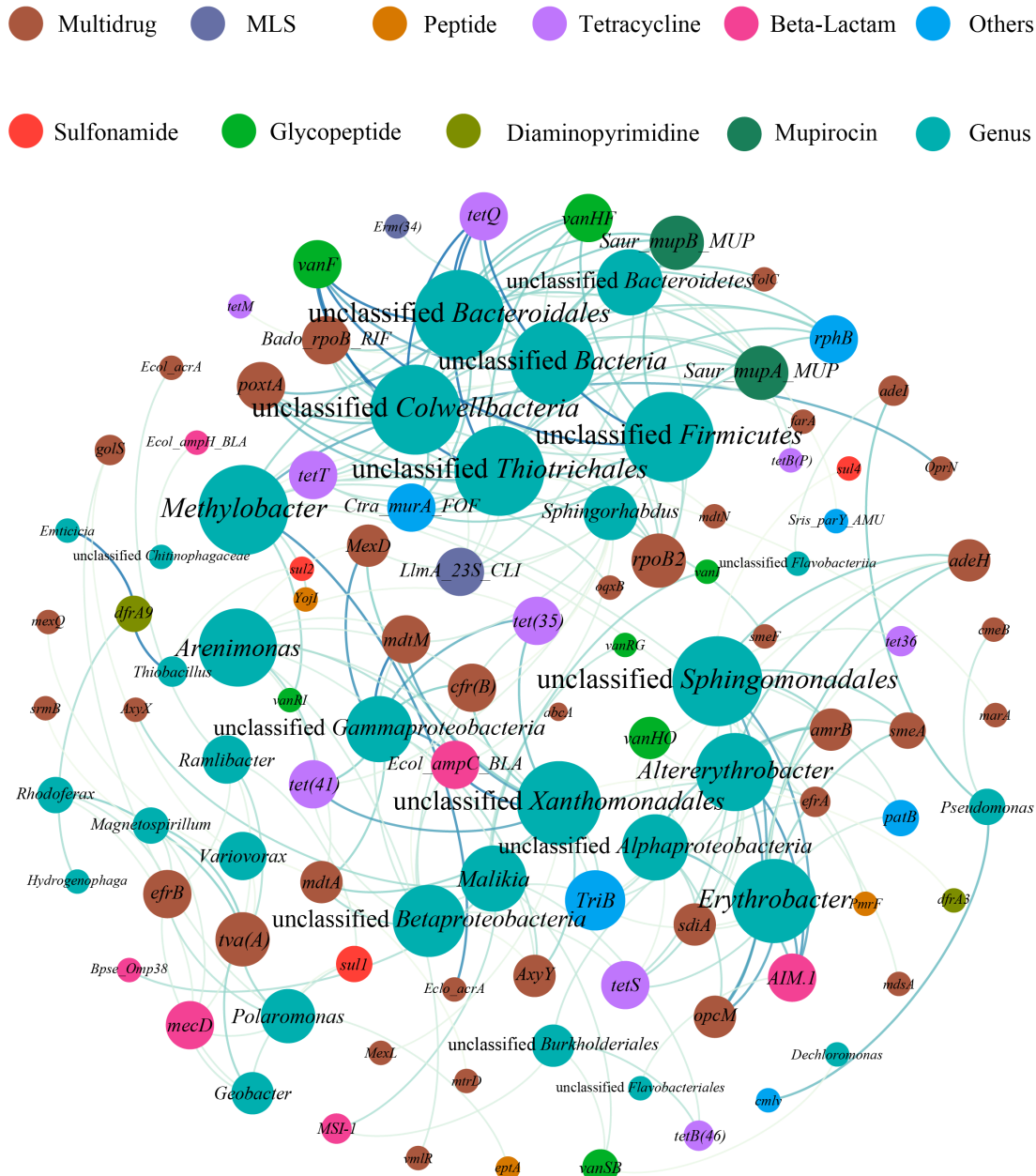
478       To investigate the associations between specific antibiotic resistance gene (ARG)  
 479 subtypes and the microbial community, a co-occurrence network analysis was

480 performed using ARG subtypes with a standardized abundance  $\geq 10$  ppm and bacterial  
481 genera with an abundance  $\geq 1000$  ppm (Fig. 11). Among the 32 bacterial genera  
482 included in the network, 23 belonged to the phylum Proteobacteria, 6 to Bacteroidetes,  
483 and one each to Firmicutes, unclassified Bacteria, and *Candidatus\_Colwellbacteria*.  
484 These findings indicate that Proteobacteria and Bacteroidetes are key microbial phyla  
485 influencing the distribution and dissemination of ARGs in the groundwater of this study  
486 area. This is consistent with the composition of the microbial community in the  
487 groundwater of the industrial park reported in the study by Xu et al. (2019).

488 We performed a network analysis on ARG subtypes with a standardized abundance  
489 of 10 ppm and bacterial genera with an abundance exceeding 1000 ppm, with the results  
490 shown in Fig. 11. Among these, the bacterial genera exhibiting the highest  
491 connectivity—unclassified Bacteroidales, *Methylobacter*, unclassified  
492 Sphingomonadales, unclassified Thiotrichales, unclassified *Colwellbacteria*, and  
493 unclassified Firmicutes—each demonstrated significant associations with 12 ARG  
494 subtypes.

495 *Methylobacter* is a genus of methanotrophic bacteria that assimilates  
496 formaldehyde via the ribulose monophosphate pathway and plays a significant role in  
497 mitigating methane emissions. However, recent studies have isolated strains of this  
498 genus from culture media supplemented with multiple antibiotics, indicating potential  
499 multidrug resistance. Coupled with the co-occurrence relationships observed in this  
500 study between *Methylobacterium* and multiple ARG subtypes, it is plausible that this  
501 genus may act as a potential host for ARGs. Therefore, when utilizing

502 Methylobacterium for methane emission reduction, attention must be given to its  
503 potential role in disseminating antibiotic resistance genes.



504 Fig. 11 Network analysis among ARG subtypes and bacteria communities at genus level in  
505 506 groundwater samples.

### 3.5 Factors influencing the spatial variation of ARGs in soil-groundwater systems

509 Numerous studies have indicated that ARGs in surface soil can migrate to deeper

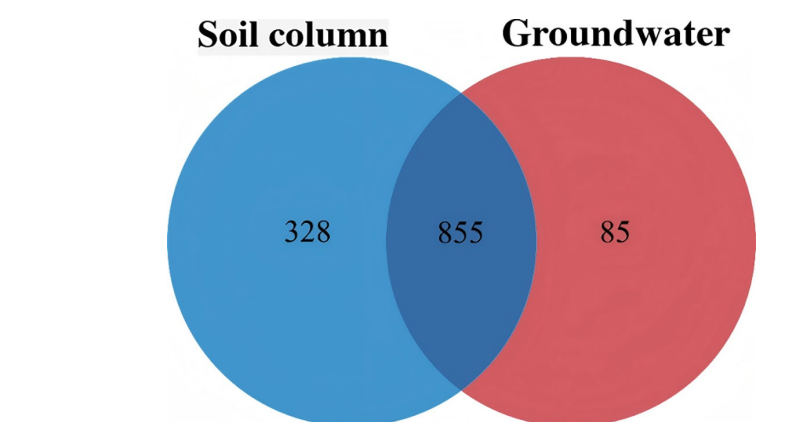
510 soil layers via vertical transport, potentially contaminating groundwater (Huang et al.,  
511 2013; Li et al., 2022a). In this study, previously obtained metagenomic data from soil  
512 cores in the industrial park were integrated with groundwater data to investigate the  
513 distribution and migration patterns of ARGs and ARBs within the soil-groundwater  
514 system. The results are presented in Fig. 12 and Fig. 13 (Miao et al., 2025).

515 Through metagenomic analysis of four paired soil-groundwater samples, 1229 and  
516 998 ARG subtypes were detected in the soil cores and groundwater, respectively.  
517 Among these, 855 subtypes (accounting for 91.0% of the total detected in groundwater)  
518 were co-present in both media. The overall abundance levels of ARGs in the two media  
519 were similar (averaging 15,814.8 ppm in soil cores and 14,587.2 ppm in groundwater),  
520 and their composition and abundance distribution exhibited high similarity. Multidrug,  
521 macrolide, glycopeptide, tetracycline, and peptide resistance genes showed high  
522 abundance in both compartments and were relatively enriched in the deep soil layer  
523 (T5). These results indicate that ARGs from deep soil layers can migrate into  
524 groundwater and persist stably over time, thereby influencing the composition of the  
525 groundwater resistome.

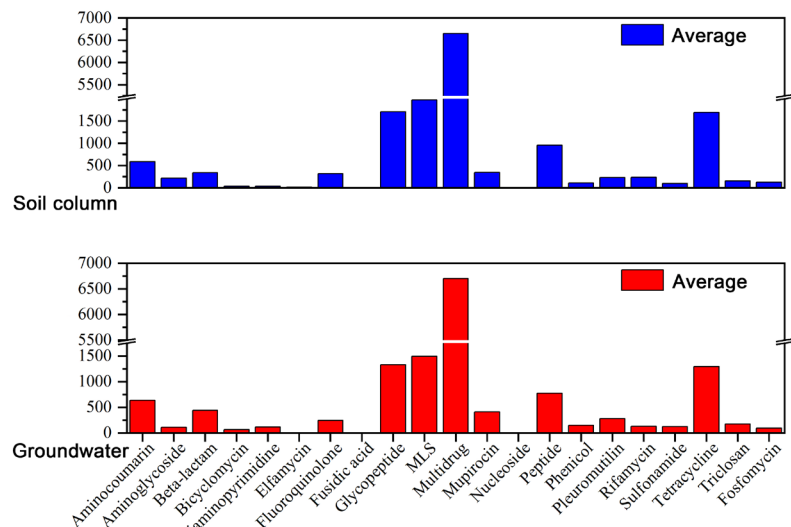
526 The study further identified the primary drivers influencing the distribution of  
527 ARGs within the soil-groundwater system, including antibiotics, heavy metals, PAHs,  
528 mobile genetic elements (MGEs), microbial communities, and environmental  
529 physicochemical properties. Among these, microbial communities are widely  
530 recognized as a key factor shaping the spatial distribution of ARGs. ARBs can facilitate  
531 long-distance transport via carriers such as soil particles and aerosols, thereby

532 participating in the global circulation of resistance genes. To clarify the specific  
533 composition of ARB in the study area, a co-occurrence network was constructed,  
534 revealing potential host relationships between 56 microbial genera and 260 ARG  
535 subtypes. This approach enabled the systematic identification of key potential ARB in  
536 the industrial park's soil-groundwater system.

537  
538  
539



540  
541 Fig. 12 Distribution of ARG subtypes species in soil columns and groundwater samples.  
542



543  
544 Fig. 13 Comparison of normalized abundance of 21 ARGs in soil columns and groundwater  
545 samples.

546 **3.6 Environmental drivers of microbial taxa abundance**

547 The relationships between the microbial community in groundwater and  
548 antibiotics, PAHs, and physicochemical properties were explored using redundancy  
549 analysis (Fig. 14, Fig. 15, Fig. 16). The results indicate that 13 environmental factors,  
550 including multiple antibiotics (OFC, ETM, NFC, MLs, FQs, TC), PAHs (Ace, Chr, Pyr,  
551 Flu), and physicochemical parameters (pH, DOC, DO), were significantly correlated  
552 with the bacterial community structure in groundwater. Among these, contaminant  
553 factors (antibiotics and PAHs) played a predominant role, further confirming that  
554 contaminants are the key factors influencing the microbial community structure in the  
555 groundwater of this region. This finding is consistent with previous studies reporting  
556 that antibiotics and PAHs are important factors affecting the microbial community  
557 structure in groundwater (Guo et al., 2022; Sun et al., 2022).

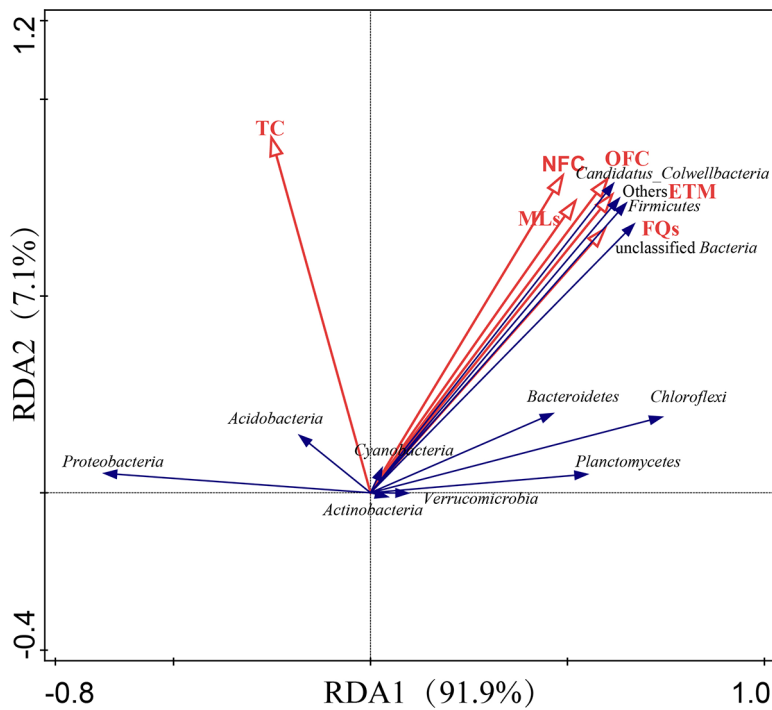
558 As shown in Fig. 14, the influence of different antibiotics on the microbial  
559 community varies. For instance, Proteobacteria exhibited a significant positive  
560 correlation solely with tetracycline, while showing significant negative correlations  
561 with norfloxacin, ofloxacin, erythromycin, fluoroquinolones, and macrolide antibiotics.  
562 PAHs alter the microbial community structure to adapt to the contaminated  
563 environment by promoting the growth of microorganisms with degradation capabilities,  
564 and the effects of different categories of PAHs on various microbial communities also  
565 differ (Sun et al., 2022). In the groundwater of the study area, Ace demonstrated the  
566 highest correlation among all PAH factors significantly associated with the microbial  
567 community, whereas Pyr and Flu showed significant positive correlations with a

568 broader range of bacterial phyla (Fig. 15).

569 Water quality parameters also influenced the microbial composition. pH and  
570 dissolved organic carbon showed significant positive correlations with major bacterial  
571 phyla, except for Proteobacteria, while dissolved oxygen was significantly positively  
572 correlated only with Proteobacteria and negatively correlated with other major phyla.  
573 These findings differ from some prior research results; variations in geographical  
574 location, groundwater physicochemical parameters, and contaminant concentration  
575 levels may account for the discrepancies in the influence of environmental factors  
576 (Xiong et al., 2022) (Fig. 16).

577

578



579  
580 Fig. 14 RDA showing the influence from antibiotics on microbial communities in groundwater.

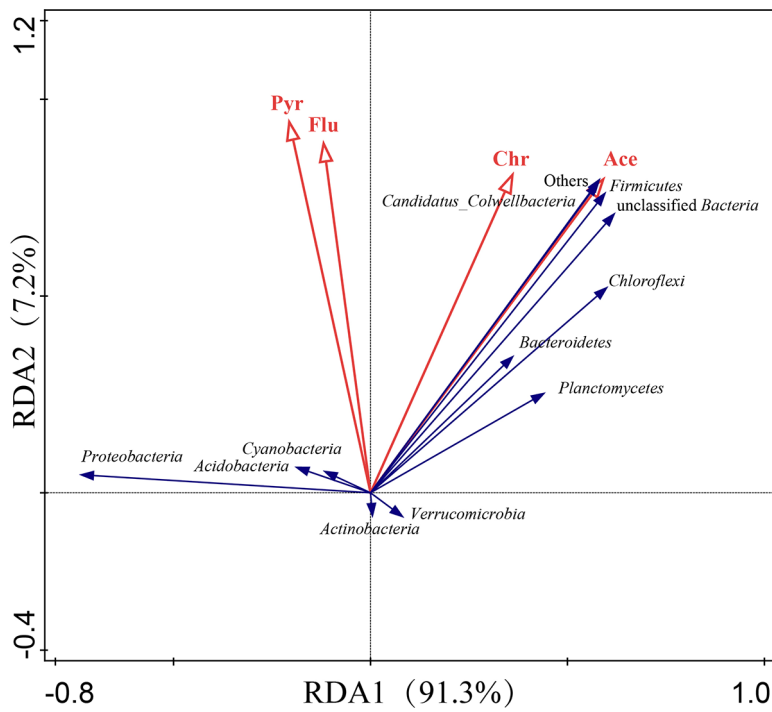


Fig. 15 RDA showing the influence from PAHs on bacteria communities in groundwater.

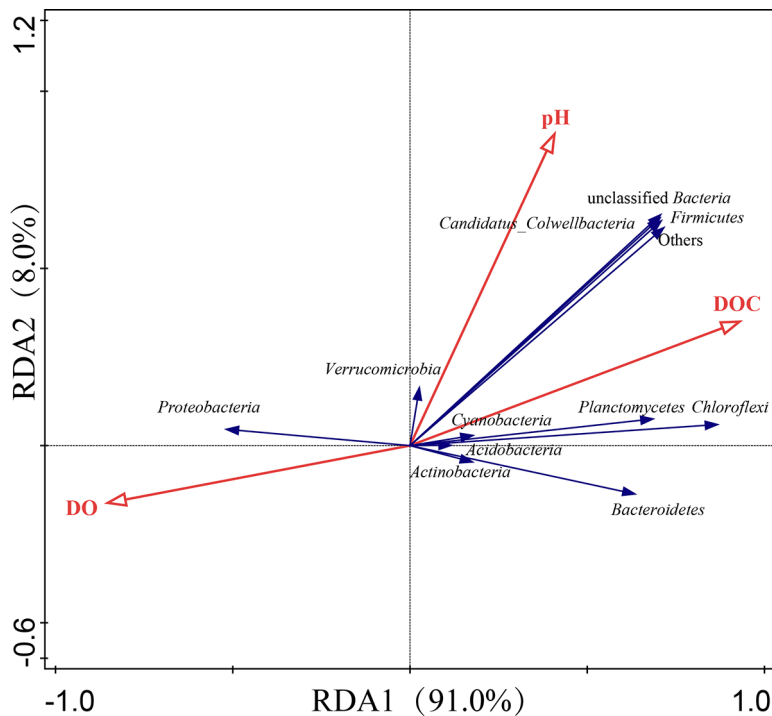


Fig. 16 RDA showing the influence from physicochemical properties on bacteria communities in groundwater.

587 **4 Discussion**

588 **4.1 Distribution and transport of antibiotics and potential controlling factors**

589 **4.1.1 Distribution and Migration of Antibiotics in Groundwater**

590 The concentration of sulfonamide antibiotics (SAs) in the groundwater of this  
591 study area is significantly higher than those reported in Hubei Province, China (Tong  
592 et al., 2020), Barcelona, Spain (Lopez-Serna et al., 2013), Guizhou Province, the  
593 Ganges Basin, India (Sharma et al., 2019), Beijing, China (Chen et al., 2017d), and  
594 Tianjin, China (Hu et al., 2010). However, it is lower than that observed in Heilongjiang  
595 Province, China (Ma et al., 2021) and similar to levels documented in North Carolina,  
596 USA (Gray et al., 2020).

597 The concentration of fluoroquinolone antibiotics (FQs) is notably higher than  
598 those reported in Beijing, China (Chen et al., 2017d), the Ganges Basin, India (Sharma  
599 et al., 2019), and Heilongjiang Province, China (Ma et al., 2021). It is lower than the  
600 level observed in Barcelona, Spain (Lopez-Serna et al., 2013) and comparable to those  
601 in Hubei Province, China (Yao et al., 2017a) and Tianjin, China (Hu et al., 2010).

602 The concentration of tetracycline antibiotics (TCs) is markedly higher than those  
603 reported in Beijing, China (Chen et al., 2017d) and Tianjin, China (Hu et al., 2010), but  
604 lower than that in Hubei Province, China (Yao et al., 2017a). It is similar to levels  
605 recorded in Barcelona, Spain (Lopez-Serna et al., 2013) and Guizhou Province.

606 Macrolide antibiotic (MLs) concentrations in the groundwater are relatively low,  
607 significantly lower than those reported in North Carolina, USA (Gray et al., 2020) and

608 Hubei Province, China (Yao et al., 2017a), and comparable to levels in Heilongjiang  
609 Province, China (Ma et al., 2021). Chloramphenicol antibiotic (CPs) concentrations are  
610 modest and similar to those reported in Tianjin, China (Hu et al., 2010).

611 Compared with surface water in other regions, the concentrations of SAs and TCs  
612 in this study area are significantly lower than those in surface water from Hubei  
613 Province (Tong et al., 2020), the Huangpu River in Shanghai (Chen and Zhou, 2014),  
614 and lake water from Hubei Province (Tong et al., 2020). The concentration of FQs is  
615 broadly similar to that in the Huangpu River, Shanghai (Chen and Zhou, 2014), but  
616 notably lower than those in surface water and lake water from Hubei Province (Tong et  
617 al., 2020). MLs concentrations are comparable to those reported in the Huangpu River,  
618 Shanghai (Chen and Zhou, 2014), as well as in surface water and lake water from Hubei  
619 Province (Tong et al., 2020). CPs concentrations are significantly lower than those  
620 reported in the Huangpu River, Shanghai (Chen and Zhou, 2014).

621 In summary, the overall antibiotic contamination level in the groundwater of the  
622 study area is moderate. Compared to surface water, the concentrations of SAs and TCs  
623 in the groundwater of this area are significantly lower than those in surface waters of  
624 Hubei (China), the Huangpu River (Shanghai), and lake waters in Hubei (China). The  
625 concentration of FQs is comparable to that in the Huangpu River (Shanghai) but notably  
626 lower than those in surface waters and lake waters of Hubei (China). The concentration  
627 of MLs is similar to those in the Huangpu River (Shanghai), surface waters of Hubei  
628 (China), and lake waters of Hubei (China), while the concentration of CPs is  
629 significantly lower than that in the Huangpu River (Shanghai). Overall, the antibiotic

630 contamination level in the groundwater of the study area is considered moderate.

631 The distribution and transport of antibiotics in groundwater are jointly regulated  
632 by multiple processes, including adsorption, biodegradation, and climatic conditions  
633 (Zainab et al., 2020). Their adsorption behavior is influenced by factors such as their  
634 physicochemical properties, initial concentration, ionic strength, temperature, and pH  
635 (Loftin et al., 2008). In groundwater, lower microbial abundance and diversity, as well  
636 as insufficient nutrients and dissolved oxygen, can inhibit the biodegradation rate of  
637 antibiotics and may even promote their transformation into more stable and harmful  
638 metabolites, leading to persistent accumulation in aquifers (Gartiser et al., 2007; Sui et  
639 al., 2015; Lapworth et al., 2012). Furthermore, climatic conditions—such as rainfall  
640 frequency and intensity—and groundwater recharge characteristics also affect the  
641 mobility of antibiotics in aquatic systems (Zainab et al., 2020). Simultaneously, the  
642 combined effects of multiple coexisting contaminants may significantly influence the  
643 transport and transformation processes of antibiotics.

644

#### 645 **4.1.2 Potential controlling factors**

646 To investigate the key factors influencing the distribution of antibiotics in  
647 groundwater, redundancy analysis was conducted between groundwater  
648 physicochemical parameters and the concentrations of five antibiotic classes (as well  
649 as total antibiotics). The results showed that dissolved organic carbon (DOC), salinity,  
650 and dissolved oxygen (DO) were significantly correlated with the concentrations of all

651 five antibiotic classes and total antibiotics. Specifically, total antibiotic concentration,  
652 along with sulfonamides (SAs), fluoroquinolones (FQs), tetracyclines (TCs), and  
653 macrolides (MLs), exhibited significant positive correlations with DOC and salinity,  
654 and negative correlations with DO. In contrast, chloramphenicols (CPs) showed a  
655 positive correlation with DO and negative correlations with DOC and salinity. These  
656 findings align with previous research, which indicates that most antibiotics degrade  
657 more readily under aerobic conditions, while chloramphenicol (a member of the CPs  
658 class) is more efficiently removed in anaerobic environments (Lai et al., 1995). This  
659 suggests that the molecular structure of antibiotics is a key determinant of their  
660 migration behavior under similar oxygen conditions. Among all significantly correlated  
661 physicochemical parameters, DOC ( $r^2 = 0.83$ ,  $p = 0.003$ ) emerged as the most  
662 influential environmental factor affecting antibiotic concentrations. DOC likely  
663 facilitates the transport and enrichment of antibiotics in groundwater by acting as a  
664 carrier for organic pollutants and providing adsorption sites (Fig. 5).

665 Furthermore, analysis of polycyclic aromatic hydrocarbon (PAH) contamination  
666 indicates that, compared to groundwater from other regions both domestically and  
667 internationally, the total concentration of 16 PAHs in the groundwater of this study area  
668 is significantly higher than those reported in Taiyuan, China (135 ng L<sup>-1</sup>) (Li et al.,  
669 2015c) and Jharkhand, India (22 ng L<sup>-1</sup>) (Ambade et al., 2021), and is similar to the  
670 level reported in Rawalpindi, Pakistan (763 ng L<sup>-1</sup>) (Saba et al., 2012), reflecting a  
671 relatively high contamination level.

672 Redundancy analysis further revealed that multiple PAH congeners, including

673 total PAHs, showed significant positive correlations with four antibiotic classes  
674 (excluding chloramphenicols) and total antibiotic concentrations, with total PAHs  
675 exhibiting the strongest correlation. Additionally, the abundance of PAH-degrading  
676 microorganisms—primarily Firmicutes and Actinobacteria—increased significantly  
677 under high PAH exposure (Yu et al., 2017; Wang et al., 2017). Through the RND efflux  
678 pump EmhABC, PAH-degrading bacteria can simultaneously expel both PAHs and  
679 antibiotics (Yao et al., 2017b). Concurrently, the presence of antibiotics in the  
680 environment can induce reactive oxygen species-mediated damage to PAH-degrading  
681 bacterial cells and significantly inhibit their PAH degradation capacity (Fig. 6).

682 Therefore, we hypothesize that the combined microbial interactions between  
683 PAHs and antibiotics in the groundwater environment may be the primary reason for  
684 the observed significant positive correlation between PAHs and antibiotics in  
685 groundwater.

## 686 **4.2 Pollution level, transfer of ARGs and inducing factors**

### 687 **4.2.1 Drivers of Groundwater Antibiotic Resistance Gene (ARG) Contamination 688 and Transfer**

689 Based on the results of redundancy analysis (RDA), the significantly correlated  
690 influencing factors with high coefficients of determination ( $r^2$ ) were categorized into  
691 three groups: environmental factors (DOC); pollutants (Ace, Flu, Pyr, TPAH, NFC,  
692 OFC, ETM, FQs, and MLs); and microbial communities (Proteobacteria, Firmicutes,  
693 Chloroflexi, *Candidatus\_Colwellbacteria*, TotalMic, and Shanno). Variance

partitioning analysis (VPA) revealed that these three categories of influencing factors collectively explained 70.9% of the variation in the distribution of ARGs in groundwater. Among them, pollutants — represented by antibiotics and PAHs — contributed the most (52.4%), serving as the primary drivers of ARG dissemination in the industrial park groundwater, followed by microbial communities (43.9%). These results indicate that pollutant inputs exert a more critical controlling role in the spread of ARGs in groundwater compared to microbial structure and environmental conditions (Fig. 17).

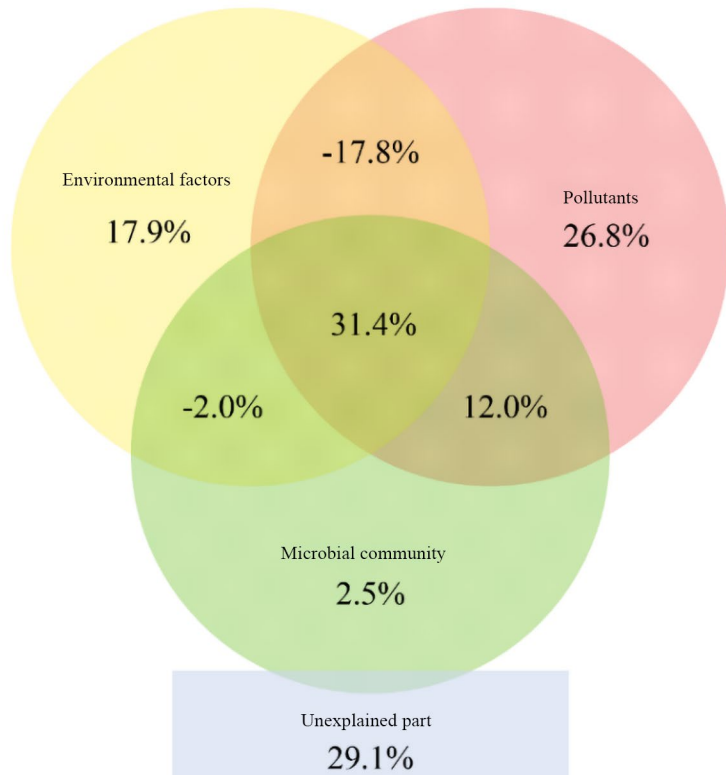


Fig. 17 Variation partitioning analysis (VPA) differentiating the effects of environmental factors, bacterial communities, and pollutants on the shift of ARGs in groundwater samples

Redundancy analysis (RDA) of the concentrations of 20 individual antibiotics, five major antibiotic classes, and total antibiotics in relation to 21 classes of ARGs in groundwater revealed significant positive correlations between tetracyclines (TCs),

708 fluoroquinolones (FQs), macrolides (MLs) and their corresponding ARG abundances,  
709 consistent with previous research (Liu et al., 2019c). On one hand, each class of  
710 antibiotics selectively inhibits the growth of susceptible bacteria, thereby providing  
711 greater survival advantages for the minority of resistant bacteria, which subsequently  
712 proliferate and accelerate the amplification and dissemination of their corresponding  
713 ARGs (Gullberg et al., 2011). On the other hand, certain bactericidal antibiotics (e.g.,  
714 fluoroquinolones) can stimulate bacterial cells to produce reactive oxygen species,  
715 triggering the SOS response and inducing resistance mutations and ARG recombination,  
716 thereby further promoting the spread of ARGs (Hughes and Andersson, 2012; Kohanski  
717 et al., 2010). Additionally, MLs exhibited the highest correlation coefficient with ARGs,  
718 likely due to their relatively low detected concentrations in the groundwater of the study  
719 area (Hughes and Andersson, 2012). Under low-level antibiotic exposure, the  
720 continuous accumulation of multiple minor phenotypic mutations may be more  
721 conducive to the enrichment of ARBs (Miao et al., 2021) (Fig. 18).

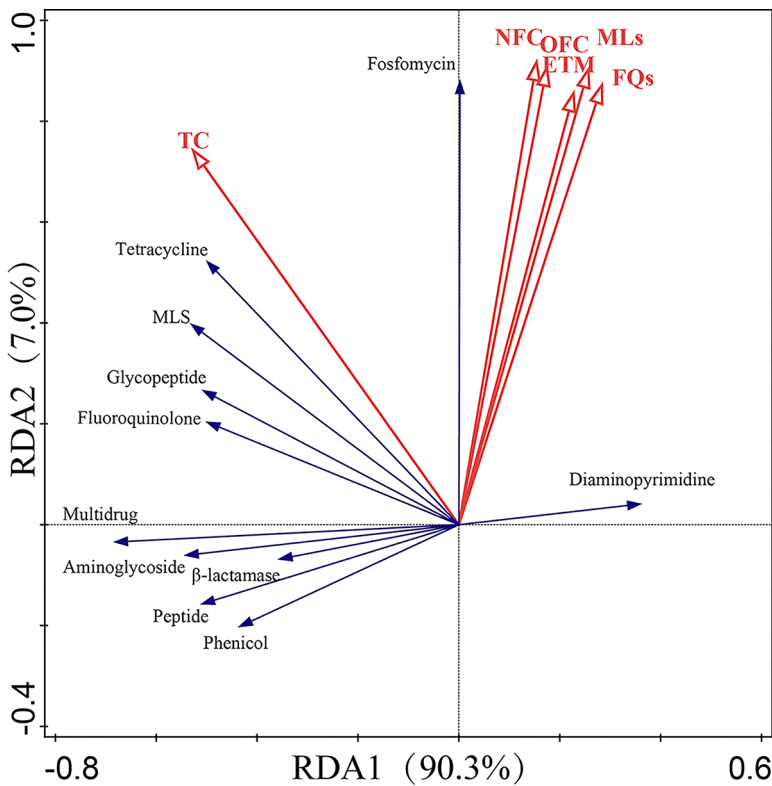


Fig. 18 RDA showing the influence from antibiotics on ARGs in groundwater samples.

722  
723  
724

725 Significant correlations between PAHs and ARGs have been confirmed in various  
726 types of soils (Azhogina et al., 2022). However, the influence of PAHs on ARG  
727 distribution in aquatic environments, particularly groundwater, remains poorly  
728 understood. In this study, redundancy analysis (RDA) was conducted on the  
729 concentrations of 16 individual PAHs and total PAHs (TPAH) in groundwater from the  
730 industrial park in relation to 21 classes of ARGs. The results showed that six PAH  
731 congeners (Ace, Phe, Flu, Pyr, BaA, Chr) and TPAH were significantly correlated with  
732 ARGs (Fig. 19). Consistent with previous studies (Wang et al., 2017), Phe, Flu, and Pyr  
733 exhibited significant positive correlations with most major ARG classes detected in  
734 groundwater, including multidrug, glycopeptide, macrolide, and tetracycline resistance  
735 genes, which may be related to the horizontal gene transfer of ARGs. Previous studies  
736 have found that 0.5 mg/L of Phe and 0.05 mg/L of Pyr significantly promoted RP4

737 plasmid-mediated horizontal transfer of ARGs by inducing elevated intracellular  
738 reactive oxygen species (ROS) levels, altering cell membrane permeability, and  
739 inhibiting mRNA expression of korA and korB genes.

740 Although TPAH showed the highest correlation coefficient with ARGs overall, it  
741 exhibited a significant negative correlation with the most dominant multidrug resistance  
742 genes in the study area. On one hand, the predominance of low-molecular-weight PAHs  
743 in the industrial park groundwater may form loosely aggregated complexes with  
744 adenine bases in plasmids via  $\pi$ - $\pi$  interactions, thereby inhibiting horizontal transfer of  
745 ARGs (Kang et al., 2015). On the other hand, higher pollutant concentrations may  
746 inhibit the survival or even cause mortality of ARBs, thus slowing the dissemination of  
747 ARGs (Qiu et al., 2012). Therefore, we hypothesize that the higher proportion of low-  
748 to medium-ring PAHs and the elevated PAH contamination levels in the groundwater  
749 of this study area may have suppressed the proliferation and spread of certain ARG  
750 classes.

751

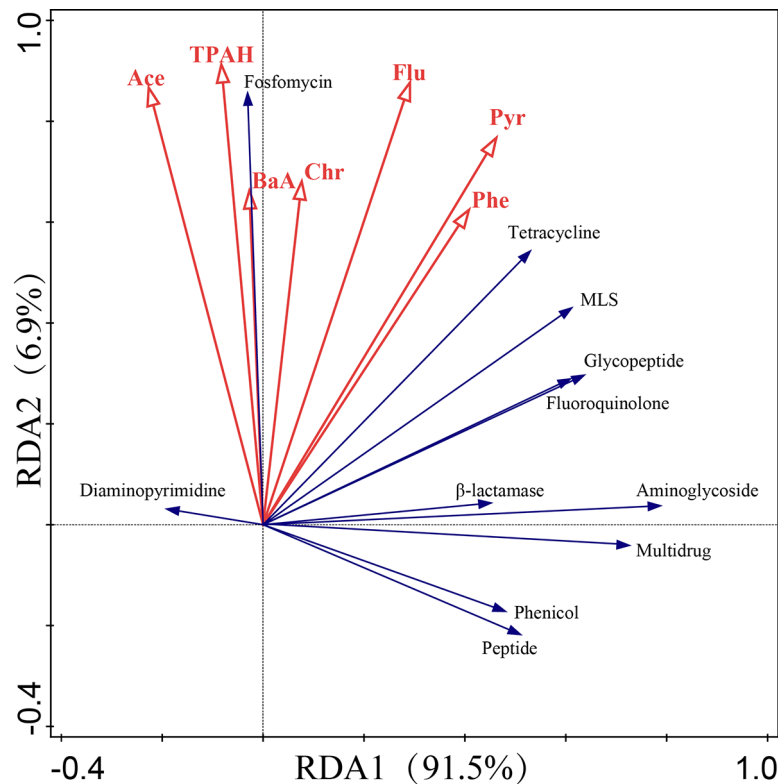


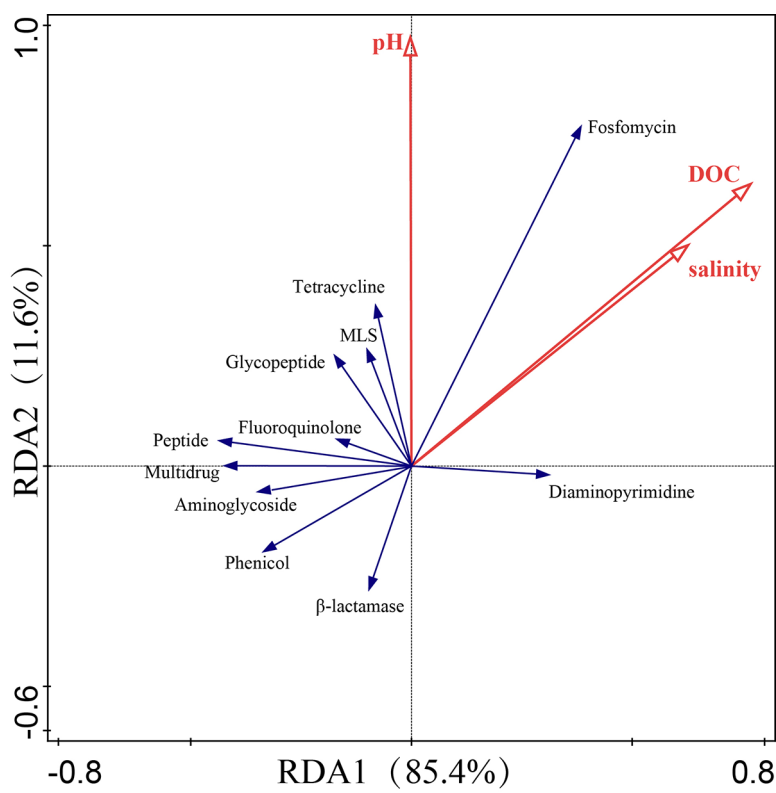
Fig. 19 RDA showing the influence from PAHs on ARGs in groundwater samples.

752  
753  
754

755 Redundancy analysis (RDA) indicated that environmental factors such as  
756 dissolved organic carbon (DOC), pH, and salinity in groundwater showed significant  
757 associations with the distribution of ARGs. Among these, DOC exhibited the most  
758 significant correlation, with its concentration negatively correlated with most ARGs.  
759 This finding aligns with previous studies emphasizing the notable influence of nutrient-  
760 related factors on ARGs (Gao et al., 2020). However, it contrasts with some research  
761 reporting positive correlations between ARGs and total organic carbon (TOC) or similar  
762 parameters. This discrepancy may be attributed to the unique environmental  
763 characteristics of the industrial park groundwater examined in this study: elevated  
764 levels of antibiotic and polycyclic aromatic hydrocarbon (PAH) contamination,  
765 combined with stressors such as hypoxia and oligotrophic conditions, may collectively  
766 enhance microbial stress tolerance, thereby altering the abundance and distribution

767 patterns of ARGs (Danielopol et al., 2000; Hemme et al., 2010; Yun et al., 2022). This  
768 likely explains the observed differences between groundwater in Shanghai's industrial  
769 parks and surface water bodies in Shanghai (Fig. 20).

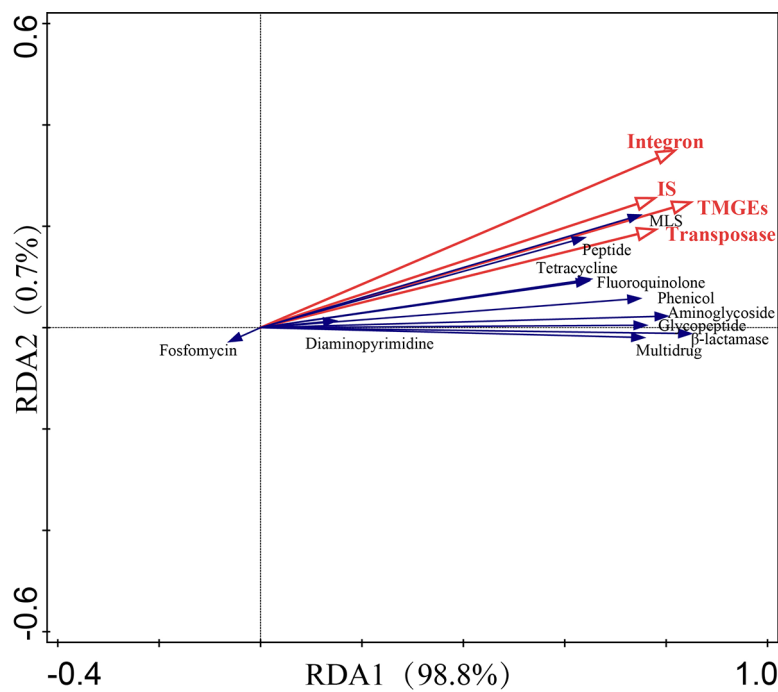
770



771  
772 Fig. 20 RDA showing the influence from physicochemical properties on ARGs in groundwater  
773 samples.

774 Mobile genetic elements (MGEs) are key drivers in the distribution and transport  
775 of ARGs in groundwater. Redundancy analysis was performed on four categories of  
776 mobile genetic elements (integrons, transposons, insertion sequences, plasmids) and  
777 total MGEs, in relation to 21 classes of antibiotic resistance genes, based on their  
778 standardized abundance. This study also conducted a correlation network analysis  
779 (Spearman's  $r > 0.6$ ,  $p < 0.01$ ) between ARG subtypes and MGEs, revealing co-  
780 occurrence patterns between ARG subtypes and MGEs in groundwater, with results  
781 shown in Fig. 22. The co-occurrence network consisted of 159 nodes (including 74

782 ARG subtypes and 85 MGEs) and 586 edges. Among these, the 85 MGEs comprised  
 783 55 transposons, 16 insertion sequences, 13 integrons, and 1 plasmid. The integron-  
 784 associated elements were the MGEs with the most connections to ARG subtypes,  
 785 showing positive correlations with 28 and 27 ARG subtypes, respectively. This  
 786 indicates that, besides transposons, integrons are also important factors in the  
 787 distribution and transport of ARGs in groundwater, which is consistent with findings  
 788 reported by Cerqueira et al (2019) (Fig. 21).



789  
 790 Fig. 21 RDA showing the influence from MGEs on ARGs in groundwater samples.  
 791

792 Redundancy analysis (RDA) demonstrated a significant association between the  
 793 microbial community structure and the distribution of ARGs in the industrial park  
 794 groundwater. Specifically, Proteobacteria and total microbial abundance (TotalMic)  
 795 were positively correlated with most major ARG classes, whereas Chloroflexi,  
 796 Planctomycetes, and the Shannon diversity index (Shanno) showed negative  
 797 correlations with dominant ARGs. These results confirm that the microbial community

798 is another critical factor—alongside pollutants, environmental parameters, and  
799 MGES— influencing the distribution and migration of ARGs in groundwater (Fig. 23).

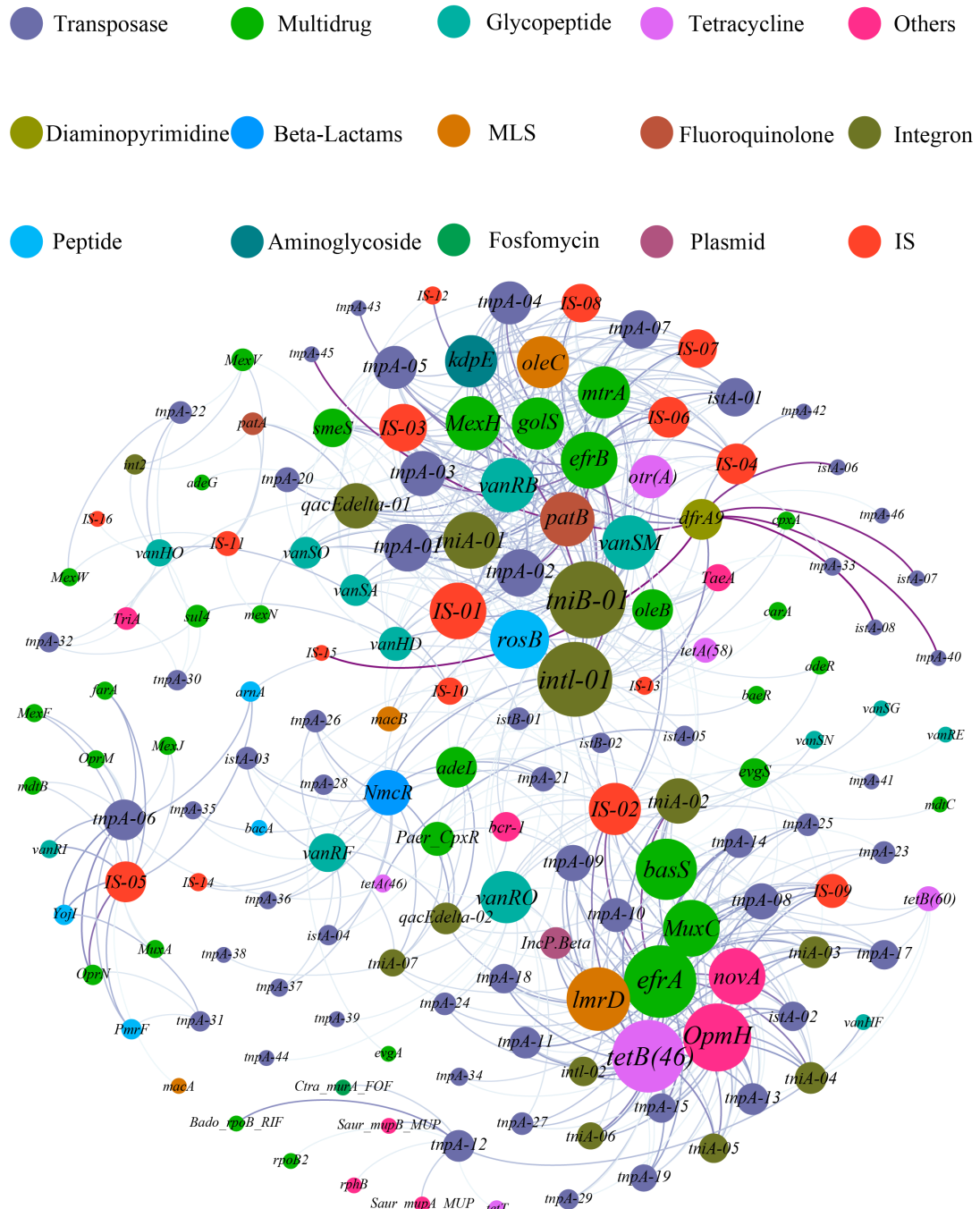
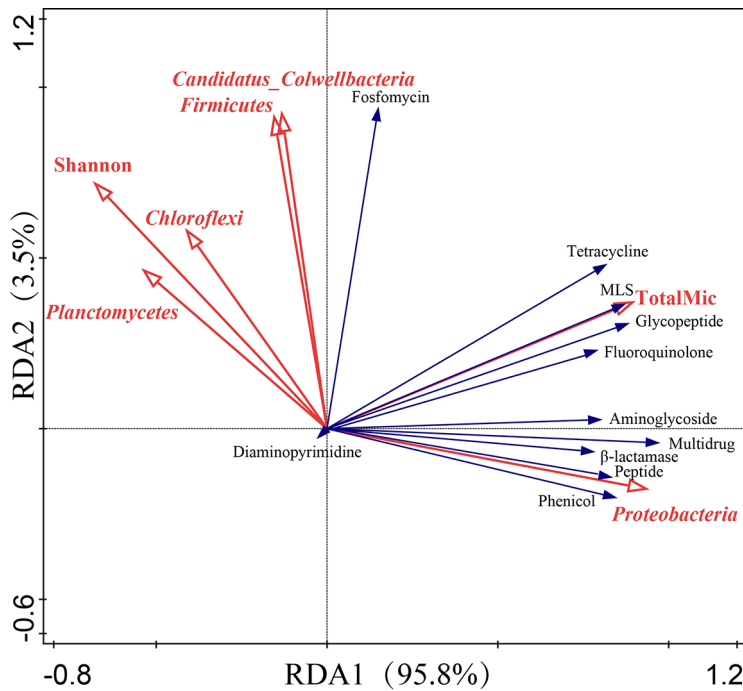


Fig. 22 Network analysis among ARG subtypes and MGEs in groundwater samples.



803  
804 Fig. 23 RDA showing the influence from microbial community on ARGs in groundwater samples.  
805

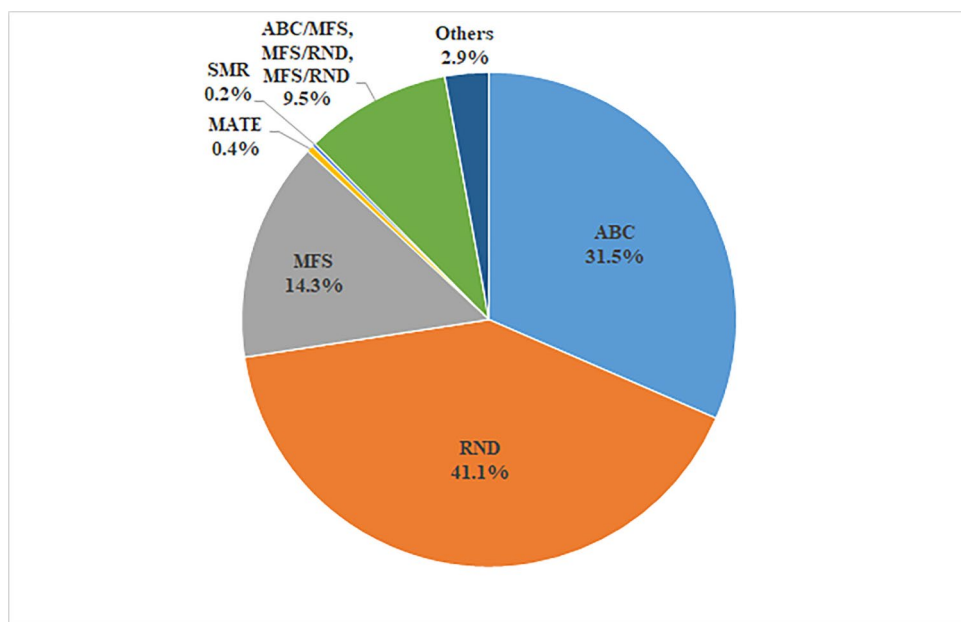
806 4.2.2 Efflux pump-mediated resistance and its role in the dissemination of antibiotic  
807 resistance genes

808 In the groundwater of the industrial park, efflux pumps constituted the dominant  
809 resistance mechanism for ARGs, accounting for an average of 65.4%, followed by  
810 antibiotic target modification (25.2%), antibiotic inactivation (4.0%), and target  
811 replacement (2.2%). This distribution aligns with findings from previous studies (Qiao  
812 et al., 2021; Yan et al., 2019). The compositional structure remained stable across most  
813 sampling sites. Among the efflux pump mechanisms, the RND type was predominant  
814 (41.1%), followed by ABC (31.5%) and MFS (14.3%) types. ARGs containing two or  
815 more efflux pump resistance mechanisms accounted for 9.5% of the total. This  
816 distribution pattern is similar to that observed in local soil cores (Miao et al., 2025).

817 The abundance and composition of ARGs were highly similar between soil cores

818 and groundwater in the industrial park. Multidrug, macrolide, glycopeptide,  
819 tetracycline, and peptide resistance genes were the dominant ARGs in the soil-  
820 groundwater system. The composition of ARG resistance mechanisms showed minimal  
821 variation between soil and groundwater, with efflux pump-based mechanisms and  
822 antibiotic target modification collectively exceeding 90% in both media. These results  
823 indicate that ARGs from soil can migrate into groundwater and persist stably over the  
824 long term, highlighting the need for focused attention on their potential risks to the  
825 groundwater environment (Fig. 24).

826



827

828

829 Fig. 24 Composition of efflux pump resistance mechanism of ARGs in groundwater samples.  
830

### 831 4.3 Distribution and transfer of pathogens

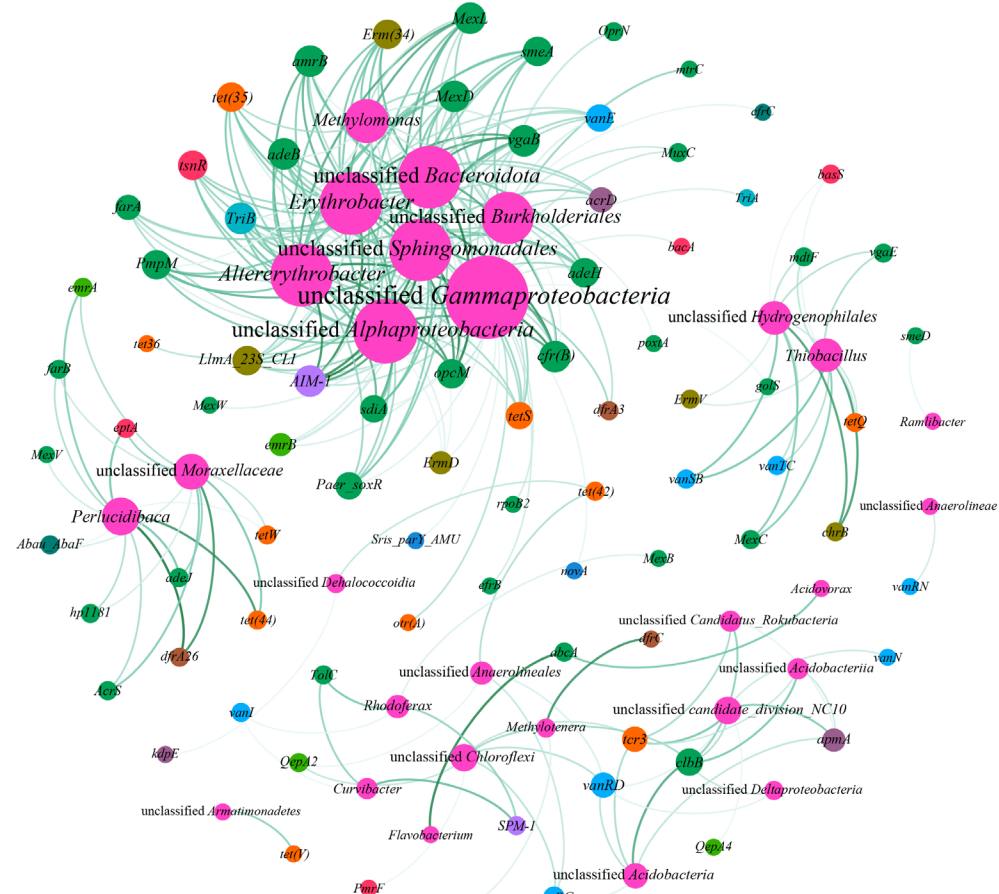
832 Co-occurrence network analysis revealed extensive associations between ARGs  
833 and bacterial genera within the soil-groundwater system of the industrial park. The

834 network comprised 109 nodes (81 ARG subtypes and 28 bacterial genera) and 265  
835 connecting edges. Taxonomically, Proteobacteria (17 genera) and Chloroflexi (4 genera)  
836 dominated the bacterial composition, indicating their roles as key potential ARBs in the  
837 distribution and migration of ARGs within the system. Among these, unclassified  
838 Gammaproteobacteria exhibited the broadest connectivity, linking to 33 ARG subtypes,  
839 while unclassified Alphaproteobacteria, unclassified Bacteroidota, Erythrobacter, and  
840 other genera also showed significant correlations with more than 10 ARG subtypes.  
841 Notably, by comparing potential hosts in soil and groundwater, seven shared bacterial  
842 genera were identified, including unclassified Burkholderiales, Thiobacillus, and  
843 Arenimonas. This suggests that these bacteria may carry ARGs and migrate vertically  
844 along the soil profile into groundwater. Thus, the vertical migration of antibiotic-  
845 resistant bacteria in the soil-groundwater system represents a critical pathway  
846 contributing to ARG contamination in groundwater (Fig. 25).

847

● Multidrug ● MLS ● Peptide ● Tetracycline ● Others ● Genus ● Diaminopyrimidine

● Glycopeptide ● Fluoroquinolone ● Beta-Lactams ● Triclosan ● Aminoglycoside ● Aminocoumarin



848

849

850 Fig. 25 Network analysis among ARG subtypes and bacteria communities at genus level in soil-  
851 groundwater system.

852

## 853 5 Conclusions

854 This study highlights the critical yet often overlooked risk posed by the vertical  
855 migration of antibiotics, ARGs, and potential pathogens in urban groundwater systems,  
856 which are simultaneously contaminated by multiple pollutants. Our findings  
857 demonstrate that the distribution and transport of antibiotics in groundwater are

858 governed by a combination of anthropogenic inputs, the physicochemical properties of  
859 antibiotics, groundwater parameters, and interactions with co-occurring contaminants.  
860 Sulfonamides were identified as the predominant antibiotic class in groundwater,  
861 whereas fluoroquinolones exhibited higher enrichment in soil, likely due to their  
862 polar/ionic functional groups and strong adsorption to soil matrices, which limit their  
863 leaching into groundwater. Vertically, antibiotic concentrations decreased exponentially  
864 with depth, with tetracyclines showing greater mobility than sulfonamides.

865 The composition and relative abundance of 21 ARG classes were highly similar  
866 between soil cores and groundwater, indicating active exchange and migration of ARGs  
867 across the soil-groundwater interface. In groundwater, contaminants—particularly  
868 antibiotics and PAHs—were the primary drivers of ARG distribution, followed by the  
869 structure of microbial communities. Mobile genetic elements (MGEs) and groundwater  
870 physicochemical parameters also played significant roles in shaping the dissemination  
871 of ARGs.

872 Integrating earlier research on ARG-hosting microorganisms in soil layers, a  
873 comparison of potential hosts in soil and groundwater identified seven shared bacterial  
874 genera, including unclassified Burkholderiales, Thiobacillus, and Arenimonas. This  
875 suggests that these bacteria may act as vectors carrying ARGs along the soil profile into  
876 groundwater. Consequently, the vertical migration of antibiotic-resistant bacteria (ARB)  
877 through the soil-groundwater continuum represents a key pathway contributing to ARG  
878 contamination in groundwater.

879 This work reveals interconnected pollution patterns in urban soil-groundwater

880 systems, where antibiotics, PAHs, and ARGs interact across deeper soil layers and  
881 groundwater, collectively threatening ecosystem security. Effective control of ARG  
882 dissemination will require integrated management strategies targeting co-pollutants  
883 such as PAHs and antibiotics to mitigate their selective pressure and reduce the spread  
884 of resistance determinants.

885 **Declaration of Competing Interest**

886 The authors declare that they have no known competing financial interests or personal  
887 relationships that could have appeared to influence the work reported in this paper.

888 **Acknowledgements**

889 This work was supported by the National Youth Key R&D Program of China [grant  
890 number 2022YFC3105800], National Natural Science Foundation of China [grant  
891 numbers 42071134, 42230505], National Key R&D Program of China [grant number  
892 2020YFC1806700]. We acknowledge our group members for their generous help in  
893 laboratory assistance.

894

895 **References**

896 Ambade B, Sethi S S, Kumar A, et al. Health risk assessment, composition, and distribution of PAHs in  
897 drinking water of southern Jharkhand, east India[J]. Archives of Environmental Contamination  
898 and Toxicology, 2021, 80: 120-133.

899 Azhogina T, Sazykina M, Konstantinova E, et al. Bioaccessible PAH influence on distribution of  
900 antibiotic resistance genes and soil toxicity of different types of land use[J]. Environmental  
901 Science and Pollution Research, 2022, 30: 12695–12713.

902 Bu Q W, Zhang Z H, Lu S, et al. Vertical distribution and environmental significance of PAHs in soil  
903 profiles in Beijing, China[J]. Environmental Geochemistry and Health, 2009, 31: 119-131.

904 Buchfink B, Reuter K, Drost H-G. Sensitive protein alignments at tree-of-life scale using DIAMOND[J].  
905 Nature Methods, 2021, 18: 366–368.

906 Buchfink B, Xie C, Huson D H. Fast and sensitive protein alignment using DIAMOND[J]. Nature  
907 Methods, 2015, 12: 59-60.

908 Cerqueira F, Matamoros V, Bayona J, et al. Antibiotic resistance genes distribution in microbiomes from  
909 the soil-plant-fruit continuum in commercial *Lycopersicon esculentum* fields under different

910 agricultural practices[J]. *Science of the Total Environment*, 2019, 652: 660-670.

911 Chen J, Yang Y, Jiang X, et al. Metagenomic insights into the profile of antibiotic resistomes in sediments  
912 of aquaculture wastewater treatment system[J]. *Journal of Environmental Sciences*, 2022a, 113:  
913 345-355.

914 Chen K, Zhou J L. Occurrence and behavior of antibiotics in water and sediments from the Huangpu  
915 River, Shanghai, China[J]. *Chemosphere*, 2014, 95: 604-612.

916 Chen S, Zhou Y, Chen Y, et al. fastp: an ultra-fast all-in-one FASTQ preprocessor[J]. *Bioinformatics*,  
917 2018, 34: 884-890.

918 Chen W-P, Peng C-W, Yang Y, et al. Distribution characteristics and risk analysis of antibiotic in the  
919 groundwater in Beijing[J]. *Environmental Science*, 2017d, 38: 5074-5080.

920 Danielopol D L, Pospisil P, Rouch R. Biodiversity in groundwater: a large-scale view[J]. *Trends in  
921 Ecology & Evolution*, 2000, 15: 223-224.

922 Das N, Kotoky R, Maurya A P, et al. Paradigm shift in antibiotic-resistome of petroleum hydrocarbon  
923 contaminated soil[J]. *Science of the Total Environment*, 2021, 757: 143777.

924 Fang P, Xiao P, Tan F, et al. Biogeographical patterns of bacterial communities and their antibiotic  
925 resistomes in the inland waters of southeast China[J]. *Microbiology Spectrum*, 2022, 10:  
926 e00406-00422.

927 Fernanda P A, Liu S, Yuan T, et al. Diversity and abundance of antibiotic resistance genes and their  
928 relationship with nutrients and land use of the inflow rivers of Taihu Lake[J]. *Frontiers in  
929 Microbiology*, 2022, 13: 1009297.

930 Fu L, Niu B, Zhu Z, et al. CD-HIT: accelerated for clustering the next-generation sequencing data[J].  
931 *Bioinformatics*, 2012, 28: 3150-3152.

932 Gao F-Z, Zou H-Y, Wu D-L, et al. Swine farming elevated the proliferation of *Acinetobacter* with the  
933 prevalence of antibiotic resistance genes in the groundwater[J]. *Environment International*,  
934 2020, 136: 105484.

935 Garcia-Galan M J, Garrido T, Fraile J, et al. Application of fully automated online solid phase extraction-  
936 liquid chromatography-electrospray-tandem mass spectrometry for the determination of  
937 sulfonamides and their acetylated metabolites in groundwater[J]. *Analytical and Bioanalytical  
938 Chemistry*, 2011, 399: 795-806.

939 Gartiser S, Urich E, Alexy R, et al. Ultimate biodegradation and elimination of antibiotics in inherent  
940 tests[J]. *Chemosphere*, 2007, 67: 604-613.

941 Gray A D, Todd D, Hershey A E. The seasonal distribution and concentration of antibiotics in rural  
942 streams and drinking wells in the piedmont of North Carolina[J]. *Science of the Total  
943 Environment*, 2020, 710: 136286.

944 Gullberg E, Cao S, Berg O G, et al. Selection of resistant bacteria at very low antibiotic concentrations[J].  
945 *Plos Pathogens*, 2011, 7: e1002158.

946 Guo Z, Wang X, Xiang S, et al. Distribution characteristics of typical antibiotics in reclaimed water  
947 infiltration area and influencing factors of groundwater microbial community[J]. *Rock and  
948 Mineral Analysis*, 2022, 41: 451-462.

949 Hao Y-L, Li G, Xiao Z-F, et al. Distribution and influence on the microbial ecological relationship of  
950 antibiotic resistance genes in soil at a watershed scale[J]. *Sustainability*, 2021, 13: 9748.

951 He P, Wu Y, Huang W, et al. Characteristics of and variation in airborne ARGs among urban hospitals  
952 and adjacent urban and suburban communities: A metagenomic approach[J]. *Environment  
953 International*, 2020, 139: 105625.

954 Hemme C L, Deng Y, Gentry T J, et al. Metagenomic insights into evolution of a heavy metal-  
955 contaminated groundwater microbial community[J]. *Isme Journal*, 2010, 4: 660-672.

956 Hu X, Zhou Q, Luo Y. Occurrence and source analysis of typical veterinary antibiotics in manure, soil,  
957 vegetables and groundwater from organic vegetable bases, northern China[J]. *Environmental*  
958 *Pollution*, 2010, 158: 2992-2998.

959 Huang F-Y, Chen Q-L, Zhang X, et al. Dynamics of antibiotic resistance and its association with bacterial  
960 community in a drinking water treatment plant and the residential area[J]. *Environmental*  
961 *Science and Pollution Research*, 2021, 28: 55690-55699.

962 Huang X, Liu C, Li K, et al. Occurrence and distribution of veterinary antibiotics and tetracycline  
963 resistance genes in farmland soils around swine feedlots in Fujian Province, China[J].  
964 *Environmental Science and Pollution Research*, 2013, 20: 9066-9074.

965 Huang Y-H, Liu Y, Du P-P, et al. Occurrence and distribution of antibiotics and antibiotic resistant genes  
966 in water and sediments of urban rivers with black-odor water in Guangzhou, South China[J].  
967 *Science of the Total Environment*, 2019b, 670: 170-180.

968 Hughes D, Andersson D I. Selection of resistance at lethal and non-lethal antibiotic concentrations[J].  
969 *Current Opinion in Microbiology*, 2012, 15: 555-560.

970 Jia B, Raphenya A R, Alcock B, et al. CARD 2017: expansion and model-centric curation of the  
971 comprehensive antibiotic resistance database[J]. *Nucleic Acids Research*, 2017, 45: D566-D573.

972 Jong M C, Harwood C R, Blackburn A, et al. Impact of redox conditions on antibiotic resistance  
973 conjugative gene transfer frequency and plasmid fate in wastewater ecosystems[J].  
974 *Environmental Science and Technology*, 2020, 54: 14984-14993.

975 Kang F, Hu X, Liu J, et al. Noncovalent binding of polycyclic aromatic hydrocarbons with genetic bases  
976 reducing the in vitro lateral transfer of antibiotic resistant genes[J]. *Environmental Science and*  
977 *Technology*, 2015, 49: 10340-10348.

978 Kohanski M A, Depristo M A, Collins J J. Sublethal antibiotic treatment leads to multidrug resistance  
979 via radical-induced mutagenesis[J]. *Molecular Cell*, 2010, 37: 311-320.

980 Lai H-T, Liu S-M, Chien Y-H. Transformation of chloramphenicol and oxytetracycline in aquaculture  
981 pond sediments[J]. *Journal of Environmental Science and Health Part A Environmental Science*  
982 and Engineering and Toxic and Hazardous Substance Control, 1995, 30: 1897-1923.

983 Lapworth D J, Baran N, Stuart M E, et al. Emerging organic contaminants in groundwater: A review of  
984 sources, fate and occurrence[J]. *Environmental Pollution*, 2012, 163: 287-303.

985 Li D, Liu C-M, Luo R, et al. MEGAHIT: an ultra-fast single-node solution for large and complex  
986 metagenomics assembly via succinct de Bruijn graph[J]. *Bioinformatics*, 2015b, 31: 1674-1676.

987 Li H, Zheng X, Tan L, et al. The vertical migration of antibiotic-resistant genes and pathogens in soil and  
988 vegetables after the application of different fertilizers[J]. *Environmental Research*, 2022a, 203:  
989 111884.

990 Li J, Zhang C, Wang Y, et al. Pollution characteristics and distribution of polycyclic aromatic  
991 hydrocarbons and organochlorine pesticides in groundwater at xiaodian sewage irrigation area,  
992 Taiyuan City[J]. *Environmental Science*, 2015c, 36: 172-178.

993 Li N, Chen J G, Liu C, et al. Cu and Zn exert a greater influence on antibiotic resistance and its transfer  
994 than doxycycline in agricultural soils[J]. *Journal of Hazardous Materials*, 2022c, 423: 127042.

995 Li R, Yu C, Li Y, et al. SOAP2: an improved ultrafast tool for short read alignment[J]. *Bioinformatics*,  
996 2009, 25: 1966-1967.

997 Li W, Liu Z S, Hu B L, et al. Co-occurrence of crAssphage and antibiotic resistance genes in agricultural

998 soils of the Yangtze River Delta, China[J]. Environment International, 2021, 156: 106620.

999 Liu X, Zhang G, Liu Y, et al. Occurrence and fate of antibiotics and antibiotic resistance genes in typical  
1000 urban water of Beijing, China[J]. Environmental Pollution, 2019c, 246: 163-173.

1001 Loftin K A, Adams C D, Meyer M T, et al. Effects of ionic strength, temperature, and pH on degradation  
1002 of selected antibiotics[J]. Journal of Environmental Quality, 2008, 37: 378-386.

1003 Lopez-Serna R, Jurado A, Vazquez-Sune E, et al. Occurrence of 95 pharmaceuticals and transformation  
1004 products in urban groundwaters underlying the metropolis of Barcelona, Spain[J].  
1005 Environmental Pollution, 2013, 174: 305-315.

1006 Lu C, Li C, Chen L. The correlation of size distribution and gas/particle partitioning of atmospheric  
1007 PAHs[J]. China Environmental Science, 2006, 26: 153-156.

1008 Ma J, Wang Z, Zhang Z, et al. Distribution characteristics of 29 antibiotics in groundwater in Harbin[J].  
1009 Rock and Mineral Analysis, 2021, 40: 944-953.

1010 Miao S, Chen L, Zuo J-E. Correlation analysis among environmental antibiotic resistance genes  
1011 abundance, antibiotics concentrations, and heavy metals concentrations based on Web of  
1012 Science searches[J]. Environmental Science, 2021, 42: 4925-4932.

1013 Noguchi H, Park J, Takagi T. MetaGene: prokaryotic gene finding from environmental genome shotgun  
1014 sequences[J]. Nucleic Acids Research, 2006, 34: 5623-5630.

1015 Norback D, Lu C, Zhang Y, et al. Sources of indoor particulate matter (PM) and outdoor air pollution in  
1016 China in relation to asthma, wheeze, rhinitis and eczema among pre-school children: Synergistic  
1017 effects between antibiotics use and PM10 and second hand smoke[J]. Environment International,  
1018 2019, 125: 252-260.

1019 Pan X, Qiang Z, Ben W, et al. Residual veterinary antibiotics in swine manure from concentrated animal  
1020 feeding operations in Shandong Province, China[J]. Chemosphere, 2011, 84: 695-700.

1021 Parnanen K, Karkman A, Hultman J, et al. Maternal gut and breast milk microbiota affect infant gut  
1022 antibiotic resistome and mobile genetic elements[J]. Nature Communications, 2018, 9: 3891.

1023 Pehrsson E C, Tsukayama P, Patel S, et al. Interconnected microbiomes and resistomes in low-income  
1024 human habitats[J]. Nature, 2016, 533: 212-216.

1025 Qiao L, Liu X, Zhang S, et al. Distribution of the microbial community and antibiotic resistance genes  
1026 in farmland surrounding gold tailings: A metagenomics approach[J]. Science of the Total  
1027 Environment, 2021, 779: 146502.

1028 Qiao M, Ying G G, Singer A C, et al. Review of antibiotic resistance in China and its environment[J].  
1029 Environment International, 2018, 110: 160-172.

1030 Qiu Z, Yu Y, Chen Z, et al. Nanoalumina promotes the horizontal transfer of multiresistance genes  
1031 mediated by plasmids across genera[J]. Proceedings of the National Academy of Sciences of  
1032 the United States of America, 2012, 109: 4944-4949.

1033 Saba B, Hashmi I, Awan M A, et al. Distribution, toxicity level, and concentration of PAHs in surface  
1034 soil and groundwater of Rawalpindi, Pakistan[J]. Desalination and Water Treatment, 2012, 49:  
1035 240-247.

1036 Seyoum M M, Obayomi O, Bernstein N, et al. Occurrence and distribution of antibiotics and  
1037 corresponding antibiotic resistance genes in different soil types irrigated with treated  
1038 wastewater[J]. Science of the Total Environment, 2021, 782: 146835.

1039 Sharma B M, Becanova J, Scheringer M, et al. Health and ecological risk assessment of emerging  
1040 contaminants (pharmaceuticals, personal care products, and artificial sweeteners) in surface and  
1041 groundwater (drinking water) in the Ganges River Basin, India[J]. Science of the Total

1042 Environment, 2019, 646: 1459-1467.

1043 Sui Q, Cao X, Lu S, et al. Occurrence, sources and fate of pharmaceuticals and personal care products in  
1044 the groundwater: A review[J]. Emerging Contaminants, 2015, 1: 14-24.

1045 Sun H, Chen Q, Chen W, et al. Assessment of biological community in riparian zone contaminated by  
1046 PAHs: Linking source apportionment to biodiversity[J]. Science of the Total Environment, 2022,  
1047 851: 158121.

1048 Tiimub B M, Zhou Z-C, Meng L-X, et al. High-Throughput profiling of the antibiotic resistance gene  
1049 transmission in aquaculture systems[J]. Environmental Engineering Science, 2022, 39: 460-473.

1050 Tong L, Qin L, Guan C, et al. Antibiotic resistance gene profiling in response to antibiotic usage and  
1051 environmental factors in the surface water and groundwater of Honghu Lake, China[J].  
1052 Environmental Science and Pollution Research, 2020, 27: 31995-32005.

1053 Wang J, Wang J, Zhao Z, et al. PAHs accelerate the propagation of antibiotic resistance genes in coastal  
1054 water microbial community[J]. Environmental Pollution, 2017, 231: 1145-1152.

1055 Wang Q, Lu Q, Mao D, et al. The horizontal transfer of antibiotic resistance genes is enhanced by ionic  
1056 liquid with different structure of varying alkyl chain length[J]. Frontiers in Microbiology, 2015a,  
1057 6: 864.

1058 Wei Z, Feng K, Li S, et al. Exploring abundance, diversity and variation of a widespread antibiotic  
1059 resistance gene in wastewater treatment plants[J]. Environment International, 2018, 117: 186-  
1060 195.

1061 Wu S, Liu X, Liu M, et al. Sources, influencing factors and environmental indications of PAH pollution  
1062 in urban soil columns of Shanghai, China[J]. Ecological Indicators, 2018, 85: 1170-1180.

1063 Xiong G, Wu J, Yang Y, et al. Microbial fields and multi-field coupling in organic contaminated  
1064 soilgroundwater systems[J]. Earth Science Frontiers, 2022, 29: 189-199.

1065 Xu X, Liu F, Xue Y-G, et al. Bacterial community structure and its influence factors of the groundwater  
1066 in an industry park[J]. Journal of Ecology and Rural Environment, 2019, 35: 255-263.

1067 Yan Z Z, Chen Q L, Zhang Y J, et al. Antibiotic resistance in urban green spaces mirrors the pattern of  
1068 industrial distribution[J]. Environment International, 2019, 132: 105106.

1069 Yang Y, Jiang X T, Chai B L, et al. ARGs-OAP: online analysis pipeline for antibiotic resistance genes  
1070 detection from metagenomic data using an integrated structured ARG-database[J].  
1071 Bioinformatics, 2016a, 32: 2346-2351.

1072 Yang Y, Zhou R, Chen B, et al. Characterization of airborne antibiotic resistance genes from typical  
1073 bioaerosol emission sources in the urban environment using metagenomic approach[J].  
1074 Chemosphere, 2018, 213: 463-471.

1075 Yao L, Wang Y, Tong L, et al. Occurrence and risk assessment of antibiotics in surface water and  
1076 groundwater from different depths of aquifers: A case study at Jianghan Plain, central China[J].  
1077 Ecotoxicology and Environmental Safety, 2017a, 135: 236-242.

1078 Yao X, Tao F, Zhang K, et al. Multiple roles for two efflux pumps in the polycyclic aromatic hydrocarbon-  
1079 degrading *pseudomonas putida* Strain B6-2 (DSM 28064)[J]. Applied and Environmental  
1080 Microbiology, 2017b, 83: e01882-01817.

1081 Yi X, Lin C, Ong E J L, et al. Occurrence and distribution of trace levels of antibiotics in surface waters  
1082 and soils driven by non-point source pollution and anthropogenic pressure[J]. Chemosphere,  
1083 2019, 216: 213-223.

1084 Yu B, Tian J, Feng L. Remediation of PAH polluted soils using a soil microbial fuel cell: Influence of  
1085 electrode interval and role of microbial community[J]. Journal of Hazardous Materials, 2017,

1086 336: 110-118.

1087 Yun Y, Su T, Gui Z, et al. Stress-responses of microbes in oil reservoir under high tetracycline exposure  
1088 and their environmental risks[J]. Environmental Pollution, 2022, 315: 120355.

1089 Zainab S M, Junaid M, Xu N, et al. Antibiotics and antibiotic resistant genes (ARGs) in groundwater: A  
1090 global review on dissemination, sources, interactions, environmental and human health risks[J].  
1091 Water Research, 2020, 187: 116455.

1092 Zhang Y-J, Hu H-W, Gou M, et al. Temporal succession of soil antibiotic resistance genes following  
1093 application of swine, cattle and poultry manures spiked with or without antibiotics[J].  
1094 Environmental Pollution, 2017a, 231: 1621-1632.

1095 Zhao F, Yang L, Qiao M, et al. Environmental behavior and distribution of antibiotics in soils: A  
1096 Review[J]. Soils, 2017, 49: 428-436.

1097 Zhou X-Y, Wang Y-Z, Su J-Q, et al. Microplastics-induced shifts of diversity and abundance of antibiotic  
1098 resistance genes in river water[J]. Environmental Science, 2020, 41: 4076-4080.

1099 Miao, YP, Liu, XR, Liu, M, et al. Vertical migration of antibiotics, ARGs, and pathogens in industrial  
1100 multi-pollutant soils: Implications for environmental and public health[J]. Ecotoxicology and  
1101 environmental safety, 2025, 303:118912.

1102

1103